University of Ulm

Department of Internal Medicine II

Medical Director: Prof. Dr. Vinzenz Hombach

C-peptide promotes lesion development in a mouse model of arteriosclerosis

Thesis

presented to the Faculty of Medicine, University of Ulm,

to obtain the degree of a Doctor of Human Biology

submitted by

Dusica Vasic

from Belgrade

2010

Amtierender Dekan:	Prof. Dr. Klaus-Michael Debatin
1. Berichterstater:	Prof. Dr. Nikolaus Marx
2. Berichterstatter:	PD Dr. Franz Oswald
Tag der Promotion:	26. 02. 2010

Table of contents

Table of contents ..... **I**

Abbreviations ..... **III**

1. Introduction **1**

1.1. Atherosclerosis - an inflammatory disease 1

1.2. Insulin resistance and endothelial dysfunction 4

1.3. Animal models of atherosclerosis 6

1.4. Mouse models of atherosclerosis 7

1.4.1. Apolipoprotein E 9

1.4.2. Apolipoprotein E deficient mice 10

1.5. C – peptide 12

1.6. C-peptide and atherogenesis 15

1.6.1. C-peptide deposition in the vessel wall in early atherosclerosis 15

1.6.2. C-peptide induces the migration of the inflammatory cells 16

1.6.3. C-peptide activates intracellular signalling pathways 16

1.6.4. C-peptide induces proliferation of vascular smooth muscle cells 17

1.7. Aim of the study 18

2. Materials and Methods **19**

2.1. Instruments 19

2.2. Reagents 20

2.3. Mice and food 22

2.4. Antibodies and buffers 22

2.5.1. Avidin Biotin Method 23

2.5.2. Oil-red-O staining for lipids 24

2.5.3. Picrosirius red staining for collagen 25

2.6. Insulin Elisa assay 25

2.7. C-peptide radioimmunoassay – RIA 26

2.8. Mice treatment 28
2.8.1. Study design 28
2.8.2. Preparation procedure 29
2.8.3. Blood profile 30
2.9. Analysis 31
2.9.1. Tissue analysis 31
2.9.2. Statistical analysis 32
3. Results 33
3.1. C-peptide and blood profile 33
3.2. C-peptide deposition in early lesions of aortic arch 37
3.3. C-peptide increases inflammatory cell content in aortic arch 40
3.4. C-peptide increases smooth muscle cell content within aortic arch 44
3.5. C-peptide increases lipid content in mice 47
3.6. Effect of C-peptide on plaque formation 49
3.7. C-peptide has no effect on collagen content 51
3.8. C-peptide deposition in aortic sinus 54
3.9. C-peptide increases inflammatory cell content in aortic sinus 56
3.10. Effect of C-peptide on the smooth muscle cell content in aortic sinus 58
3.11. Effect of C-peptide on the lipid deposition in aortic sinus 60
4. Discussion 61
5. Summary 70
6. Conclusion and future work 72
7. Literature 73
Acknowledgments 88

Abbreviations

ABC	avidin-biotin complex
AEC	3-amino-9-ethylkarbazol complex
ApoE	apolipoprotein E
$ApoE^{-/-}$	apolipoprotein deficient mice
CHD	coronary heart disease
CXCR3	CXC chemokine receptor 3
Cdc42	cell division control protein 42 homolog
C-peptide	connecting peptide
EC	endothelial cell
E3L	apolipoprotein E3-Leiden transgenic mice
HDL	high-density lipoprotein
HCL	hydrochloric acid
H_2O_2	hydrogen peroxide
ICAM-1	Inter-Cellular Adhesion Molecule 1
Ig	immunoglobulin
IGF-I	insulin-like-growth factor - I
IL	interleukin
I-TAC	interferon-inducible T cell α-chemoattractant
LDL	low-density lipoprotein
$LDLR^{-/-}$	lipoprotein - receptor deficient mice
LRP	low density lipoprotein receptor-related protein
MAPK	mitogen-activated protein kinase
MCP-1	monocyte chemoattractant protein 1
MIF	monokine induced by γ-interferon
Mig	monokine induced by interferon gamma
M-CSF	macrophage -colony – stimulating factor
mm-LDL	minimally modified LDL
NO	nitric oxide
PBS	phosphate buffered saline

PDAY	Pathobiological Determinants of Atherosclerosis in Youth
PDGF	platelet-derived growth factor
PI-3K	phosphoinositid -3 kinase
pH	pleckstrin homoloy
PRR	pattern recognition receptors
RANTES	regulated on activation, normal T cell expressed and secreted
Rb	retinoblastoma protein
RIA	radioimmunoassay
rpm	rounds per minute
ScR	scavenger receptor
SMC	smooth muscle cell
TBS	tris-buffered saline
TG	triglyceride
TLR	toll-like receptor
TNF-α	tumor necrosis factor-alpha
VCAM - 1	vascular cell adhesion molecule-1
VLDL	very low density lipoprotein
VSMC	vascular smooth muscle cell

1. Introduction

1.1. Atherosclerosis - an inflammatory disease

Atherosclerosis is a disease of large or medium vessels, which is characterized by development of atherosclerotic plaques. Atherosclerosis is the primary cause of most cardiovascular diseases and their complications including coronary heart disease (CHD), ischemic gangrene, abdominal aortic aneurysms and many cases of heart failure and stroke. It represents a complex disease and many components of the vascular metabolic and immune system are involved in this process. Atherosclerotic plaques (atheromas) are asymmetric focal thickenings in the intima of the vessel wall. The onset of the disease is described by a fatty streak formation in the intima of the vessel wall consisting of lipid droplets and various immune cells. Fatty streaks are common in young individuals, where they never cause symptoms. They may progress into atheromas or disappear with time. Atherosclerotic plaque consists of necrotic core, calcified regions, foam cells (i.e. macrophages, that accumulate modified lipids), inflamed smooth muscle cells (SMCs), endothelial cells (ECs), lymphocytes and leukocytes (Ross 1999).

Hypercholesterolemia and hypertension are two major risk factors for atherosclerosis. When the plasma level of cholesterol, mainly very low density lipoprotein (VLDL) and low density lipoprotein (LDL) - infiltrates the artery wall to an extent that goes beyond the capacity for its elimination, it retains in the extracellular matrix in the vessel wall (Skalen et al. 2002). In the intima of the arterial wall, LDLs undergo certain modifications (e.g. enzymatic or non-enzymatic oxidation). Oxidative modification of LDLs might vary from minimal (mm-LDL) to high oxidation of LDLs. In dependence of the degree of oxidation, LDLs might have a different mechanism of action. For instance, only minimally-oxidised LDL might release various bioactive phospholipids that in turn can activate endothelial cells to express leukocyte adhesion molecules, such as vascular cell adhesion molecule-1 (VCAM-1) or inter cellular adhesion molecule-1 (ICAM-1) (Shih et al. 1999, Cybulsky et al. 1999; Cybulsky et al. 2001), whereas only highly-oxidised LDL can be

recognised by the macrophages scavenger receptors to be transformed into foam cells, a crucial hell-mark of atherosclerotic plaque development. The normal endothelium does not support binding of leukocytes. However, the mm-LDL induced activation of endothelial cells results in the expression of a number of leukocyte adhesion molecules, thereby initiating the first step in atherogenesis - leukocyte recruitment and their rolling on the endothelium. Beside adhesion molecules, the activated endothelium expresses several selectins, such as P-selectines and E-selectines which also allow leukocyte adherence. After the adhesion of leukocytes to the endothelium, they migrate into the intima of the vessel wall in response to chemoattractant stimuli including chemokines such as the monocyte chemoattractant protein-1 (MCP-1), RANTES and fractalkine (Zernecke et al. 2008). Chemokines are small molecules (8kDa - 14kDa) that regulate leukocyte trafficking. Chemokines transmit their pro-migratory signals through G-protein-coupled membrane receptors. These receptors initiate adhesion and motility via pertussis-toxin sensitive G-proteins (Murdoch and Finn 2000). In the intima of the arterial wall, monocytes begin to differentiate into macrophages. This process is under a tight regulation by a growth factor, produced in the inflamed intima, namely macrophage-colony–stimulating factor (M-CSF) (Yan and Hansson 2007). Macrophage differentiation is furthermore associated with upregulation of pattern recognition receptors (PRRs) for innate immunity, including scavenger receptors (ScRs) and toll-like receptors (TLRs). TLR initiates a signal cascade that leads to macrophage activation (Janeway and Medzhitov 2002), whereas, ScR mediates uptake of the highly-oxidized LDL that leads to the formation of foam cells. Lipid-laden macrophages, known as foam cells, play a central role in the pathogenesis of atherosclerotic plaques formation. Macrophage activation in atheroma leads to a release of proinflammatory cyto- and chemokines such as IL-1, IL-6, IL-12, IL-15, IL-18, TNF-α and MIF as well as vasoactive molecules such as nitric oxide and endothelins that promote replication of smooth muscle cells and formation of extracellular matrix - all those features being characteristic for more advanced atherosclerotic lesions. A family of T-cell chemoattractants such as IP-10, Mig, and I-TAC, as well as CXCR3 in the same way can regulate lymphocyte recruitment into atherosclerotic lesions (Mach et al. 1999; Zeiher et al. 1995; Ross 1999). As this inflammatory process further continues, the activated leukocytes and arterial cells realize

fibrogenic mediators that can maintain duplication of SMCs promoting more advanced atherosclerotic lesions (Ross 1999). Interferon-γ, released by activated T-lymphocytes in the plaque, might block the collagen synthesis in SMCs, thereby limiting their ability to renew the collagen. This degradation of the arterial extracellular matrix allows the penetration of SMCs through elastic laminae and enables plaque to grow (Libby et al. 1996; Libby 2000; Libby 2001). Inflammatory processes also contribute to the development of plaque rupture and thrombotic complications of the atheroma. Activated macrophages might secrete proteolytic enzymes and matrix metalloproteinases, that in turn, might degrade the matrix complex of an atherosclerotic plaque with subsequent destabilisation of the atheroma and increased risk for plaque rupture (Libby and Aikawa 2002; Jormsjö et al. 2002), which finally leads to acute clinical events.

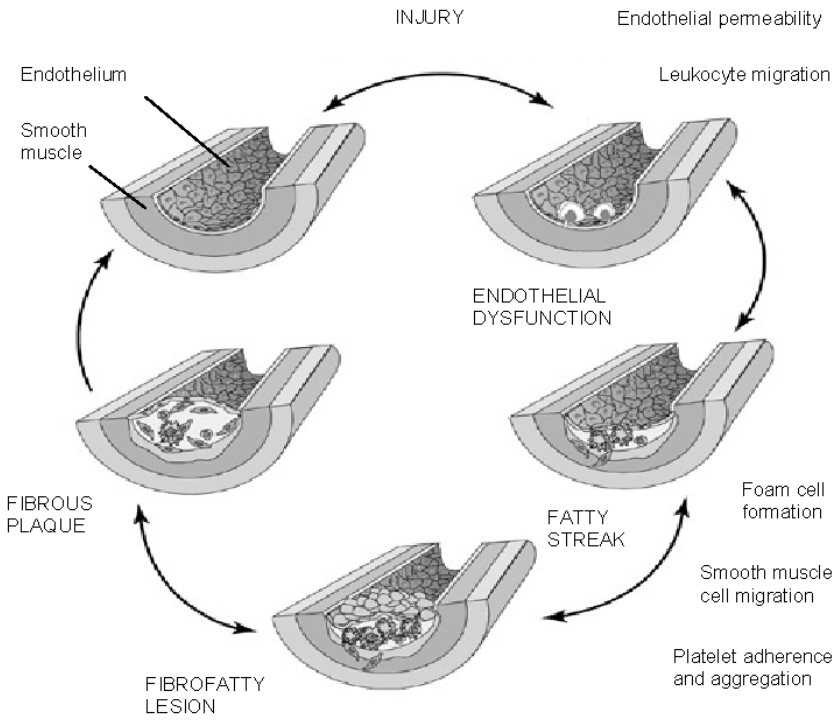

Figure 1. Atherosclerosis - an inflammatory disease (Ross 1999).

1.2. Insulin resistance and endothelial dysfunction

Individuals with diabetes have an increased risk of coronary heart disease (CHD) compared to nondiabetic individuals. The risk for a cardiovascular death for diabetic patients is as high as for non-diabetic individuals with a previous myocardial infarction (Haffner et al. 1998). Insulin resistance is a very important metabolic abnormality in type 2 diabetes, which is characterized by reduction of glucose uptake by peripheral tissues (Wheatcroft et al. 2003). Endothelial dysfunction is an important feature of glucose intolerance, diabetes, obesity, and dyslipidemia as well as a major component of cardiovascular disorders, including hypertension and atherosclerotic diseases (Reaven 1993). Insulin resistance is defined as the destruction of insulin-stimulated glucose and/or lipid metabolism, compared to the response in healthy subjects. In insulin resistant subjects a normal level of insulin does not have the same effect on muscles and adipose cells resulting in an elevated glucose level. A higher glucose level is maintained near the normal level by compensatory hyperinsulinemia. At the same time plasma levels of C-peptide are also elevated. The endothelium maintains the balance between vasodilatation and vasoconstriction, inhibition and stimulation of smooth muscle cell proliferation and migration, as well as thrombogenesis and fibrinolysis. The endothelium is a major regulator of vascular homeostasis (Kinlay et al. 2001). Endothelial dysfunction is characterized by a paradoxical or insufficient endothelial-mediated vasodilatation. Insulin resistance and endothelial dysfunction are common early findings in most asymptomatic subjects at risk for development of metabolic syndrome (Balletshofer et al. 2000). Disturbance of the balance between endothelial production of protective vasoactive molecules such as nitric oxide (NO) and the production of oxygen derived free radicals leads to a number of processes that promote atherosclerosis (Kuboki et al. 2000). Many experiments using pharmacological blockade of NO synthesis were able to reproduce an abnormal vascular response, which has been described in individuals with coronary artery disease, in individuals with multiple cardiovascular risk factors, in prediabetic subjects and in patients with type 2 diabetes mellitus (Engelke et al. 1996; Joannides et al. 1995). The majority of prediabetic and diabetic individuals who are at very high risk for the develop-

ment of coronary atherosclerosis and who have been shown to have endothelial dysfunction, also manifest moderate to severe insulin resistance (De Fronzo 1988). These results confirm that endothelial dysfunction represents a preclinical stage of atherosclerosis.

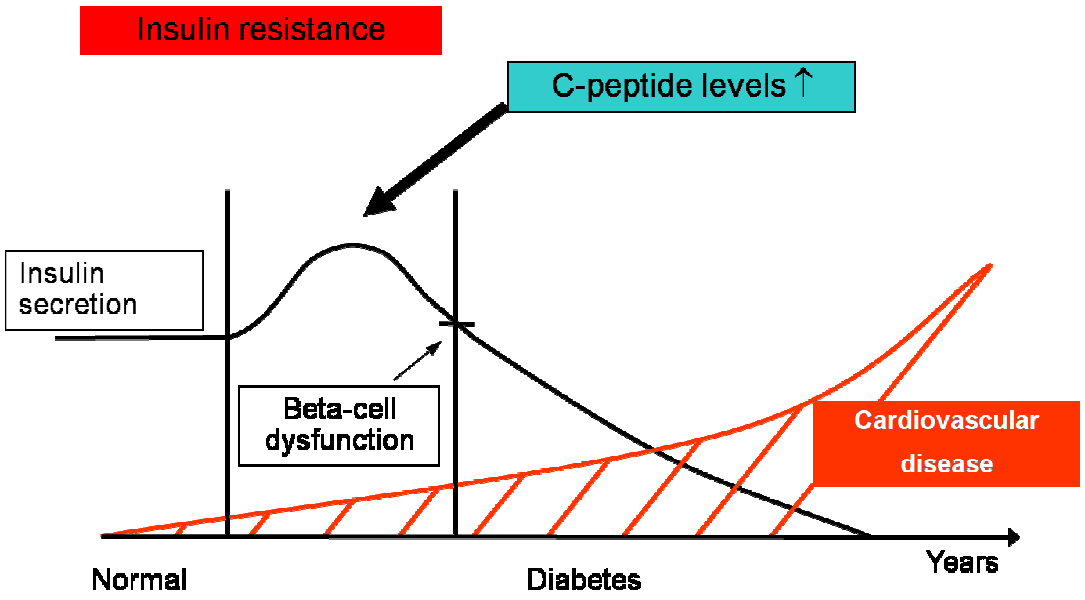

Figure 2. **Changes in insulin metabolism in the developing of type 2 diabetes.** Patients with diabetes exhibit an increased risk to develop vascular diseases with their complications such as myocardial infarction and stroke. In the period of insulin resistance blood glucose levels are maintained near normal by temporarily increased secretion of insulin. At the same time blood C-peptide levels are elevated. Recent experimental data suggest that C-peptide may play a causal role in early atherogenesis in these patients.

1.3. Animal models of atherosclerosis

The first suggestion of experimental atherosclerosis came from Ignatowski in 1908. He reported on thickening of the intima with formation of large cells in the aorta of rabbits fed with diet rich of animal proteins (Ignatowski 1908). In general, rabbits do not develop spontaneous atherosclerosis, but they are very responsive to cholesterol manipulation and develop atheroslerotic lesions in a short time. The normal range of plasma cholesterol in the New Zealand white rabbits is low (average 1.3 mmol/l), (Finking and Hanke 1997), but it could be increased by up to two to eight times after the administration of a diet with 0.1–2% cholesterol, within the first 20 days. The atherosclerotic lesions in rabbits are enriched in much more macrophages with very high levels of plasma cholesterol which is very dissimilar to human lesions (Bocan et al. 1993; Drobnik et al. 2000). Porcine models have a cardiovascular system very similar to that of humans and the chronic adaptations of the porcine coronary circulation in experimental CHD models are similar to those of human CHD patients. Pigs represent a suitable model to study the lipoprotein metabolism associated with hyperlipidemic diets, because they develop spontaneous atherosclerotic lesions even when fed with normal chow diet for a long time. When fed with high cholesterol diet, pigs reach plasma levels and atherosclerotic lesions that are similar to those seen in humans (Royo et al. 2000; Jokinen et al. 1985; Bell et al. 1992). Monkeys as a model have been well-characterized in long-term studies of primary atherosclerosis and atherosclerosis regression (Clarkson et al. 1994; Strong et al. 1994). Monkeys are not widely used because of risk of extinction and costs. Problems with pig models are costs and the difficulties involved in maintaining the colonies and handling.

1.4. Mouse models of atherosclerosis

Mice have been viewed for decades as a smart animal model of atherosclerosis for a lot of reasons. Genetic information is available on many inbreed strains which makes the task of identifying genetic links to atherosclerosis-susceptibility easier. Furthermore, small size and cost of housing mice allows greater experimental numbers to reach a statistical significant level. Mice also have a short gestation time and can multiply rapidly (Whitman 2004). However, mice are very resistant to atherosclerosis. The only exception represents the C57BL/6 mouse strain. Being fed with a very high cholesterol diet they develop lesions differing from human lesions in histological nature and location (Table 1). Piagen and colleagues modified previously the very high cholesterol diet which was toxic and made diet which consist of 15% fat, 1.25% cholesterol and 0.5% cholic acid (Paigen et al. 1985). Still, this model had a lot of disadvantages. For example the lesions were very small and limited to the aortic root usually not developing beyond the fatty-streak stage. As a truly representative model of atherogenesis, the “wild-type” mouse falls far short of other mammalian models such as non-human primates (Schwartz et al. 1985; Masuda and Ross 1990; Masuda and Ross 1990) and swine (Gerrity RG 1981; Gerrity RG 1981; Reitman et al. 1982) which both develop morphologically similar lesions reflecting all stages of the disease when compared to those found in humans.

Table 1. Selected mouse models of atherosclerosis. ApoE$^{+/-}$ mice fed with normal diet develop only the earliest stage of lesions (stage I), but feeding high cholesterol diet cause that mice develop more advanced lesions (stage III-IV) (Whitman 2004).

Mouse	Stage of lesion formed (I-IV)	Characteristics of atherosclerosis	Area of lesion characterisation	Modified diet required	Original source	Commercial availability
Inbred strains						
C57BL/6	I	Lipid-laden foam cells	Aortic root, aorta	Yes	(78, 79)	Jacksons/ Taconic/ Charles River
DBA	None		Aortic root	Yes	(79)	Jacksons/ Taconic/ Charles River
C3H	None		Aortic root	Yes	(78, 79)	Jacksons/ Taconic/ Charles River
BALB/c	None		Aortic root	Yes	(79)	Jacksons/ Taconic/ Charles River
Transgenic						
ApoB100	I-III	Lipid-laden foam cells	Aortic root	Yes	(26, 111)	Taconic
ApoE(Arg112, Cys142)	I-III	Lipid-laden foam cells	Aortic root	Yes	(25)	
ApoE3-Leiden	I-III	Lipid-laden foam cells	Aortic root	Yes	(113)	
Single Gene Replacement Human ApoE2	I-IV	Lipid-laden foam cells to lesions with necrotic core and fibrous caps	Aortic root	Yes / No	(105)	Taconic
Human ApoE3	I-III	Lipid-laden foam cells	Aortic root	Yes	(104)	Taconic
Human ApoE4	I-III	Lipid-laden foam cells	Aortic root	Yes	(45)	Taconic
Single Gene Deletion						
ApoE-/-	I-V	Lipid-laden foam cells to lesions with necrotic core and fibrous caps	Aortic root, Aorta, Innominate artery	No	(81, 82)	Jackson
ApoE+/-	I-III	Lipid-laden foam cells	Aortic root, aorta	Yes	(114,126)	Jackson
LDL receptor	I-IV	Lipid-laden foam cells to lesions with necrotic core and fibrous caps	Aortic root, aorta	Yes	(40)	Jackson

1.4.1. Apolipoprotein E

Apolipoprotein E (ApoE) is a glycoprotein, synthesized in liver, brain and other tissues in humans and mice. It is constituent of all lipoproteins except low-density lipoproteins (LDL). ApoE, is a high affinity ligand for LDL receptors and plays a crucial role in receptor-mediated uptake of all triglyceride (TG)- rich lipoprotein particles, including VLDL, chylomicrons and their residues (Mahley and Ji 1999). In this pathway, ApoE is implicated in three different uptake steps: (1) ApoE has to be bound to the surface of a lipoprotein particle to the receptor. (2) ApoE ties itself a to heparin sulphate proteoglycans to complete the ligand-receptor interaction. (3) ApoE interacts with the related protein receptor (LRP) to make the uptake process possible. Numerous abnormalities in each of these steps result in incomplete metabolism of TG-rich lipoproteins. ApoE is also synthesized in monocytes and macrophages within the vessel wall and seems to have local effect on cholesterol homeostasis and inflammatory reactions in atherosclerotic vessels (Curtiss and Boisvert 2000). The apoE gene is mapped to chromosome 19. This gene is polymorphic with three major alleles: ApoE2, ApoE3, ApoE4, which translate into three isoforms of encoding protein. These isoforms differ from each other only in one amino acid substitution with however - huge physiological effects. ApoE2 is associated with the genetic disorder called Type III hyperlipoproteinemia, which is characterized by increased plasma triglyceride and cholesterol levels and by early development of atherosclerosis. ApoE3 is considered as a physiological ApoE genotype and ApoE4 is related to atherosclerosis and Alzheimer’s disease.

1.4.2. Apolipoprotein E deficient mice

ApoE deficient mice were generated by inactivating the apoE gene. It was the first lipoprotein transport gene deleted in mice. This mouse model was developed simultaneously in two separate laboratories (Piedrahita et al. 1992; Zhang et al. 1992). Homozygous and heterozygous mice were healthy with normal development, but there are phenotypic differences between normal animals and homozygous mutants in terms of the lipoprotein profile. ApoE deficient homozygous mice on the chow diet demonstrated total cholesterol levels of more than 500 mg/dL, mostly in the VLDL and chylomicron fractions which is more than five times as much as in normal litter mates (Zhang et al. 1992; Plump et al. 1992). In general, mice demonstrate high levels of HDL and low levels of LDL compared to humans, who are high in LDL and low in HDL. It seems that mice lack cholesterol ester transfer protein, which facilitates transport of cholesterol esters and triglycerides between the lipoproteins. It collects triglycerides from very-low-density (VLDL) or low-density lipoproteins (LDL) and exchanges them for cholesterol esters from high density lipoproteins (HDL). Taking these differences into consideration, ApoE deficient mice have a phenotype very similar to ApoE deficient humans. ApoE deficient mice, fed with a normal mouse chow diet, develop foam cell accumulations on their aortic walls by three months of age, which progress to widespread atherosclerotic lesions and severe vessel occlusions by eight months (Zhang et al. 1992). At six to ten weeks of age most ApoE deficient mice develop fatty streak lesions. These fatty streak lesions progress to advanced lesions and typically consist of a necrotic core surrounded by proliferating smooth muscle cells and an extracellular matrix including collagen and elastin. These lesions have fibrous caps made of smooth muscle cells and an extracellular matrix and they often have groups of foam cells at their shoulders. Many of these lesions found in older mice develop calcified foci (Reddick et al. 1994).

A more physiological diet than the Paigen diet is called ‘Western type diet’. It consists of 21% fat, 0.15% cholesterol and no cholic acid. The ApoE deficient mouse model responds appropriately to a western type diet by developing atherosclerotic lesions (Yutaka et al. 1994).

ApoE deficient mice tend to develop extensive lesions at the base of the valve, throughout the thoracic and abdominal aortas, in the aortic bifurcation, carotid and pulmonary arteries. In each case, the lesions appeared principally at branch points, at outflow tracts or at bifurcations. In addition, they are formed on the less curvature of the arch of the aorta. These lesions also form and progress in these mice on a chow diet but in much longer time.

Development of genetically engineered mice with disorders of the lipid metabolism was a major step forward in animal models of atherosclerosis. These mice develop atherosclerosis spontaneously, which can be accelerated on a high cholesterol diet. The plaques are wider spread, reproducible and have some architectural features reminiscent to human lesions. The major difference has been that lesions occur at sites very different from human lesions – for example the aortic root and thoracic aorta (Smith et al. 1997). Despite these differences, ApoE deficient mice have very similar characteristics of the disease to those of ApoE deficient humans (Jawien et al. 2004). The complexity of lesion in ApoE deficient mice together with the advantage of using the mouse model in human disease, makes it an attractive system to study environmental and genetic features of the disease.

1.5. C – peptide

C-peptide represents a 31 amino acid peptide cleaved from proinsulin (Figure 3). Proinsulin consists of an A-chain, a connecting peptide (C-peptide), and a B-chain (Rubenstein et al 1969). After proinsulin cleavage within the endoplasmatic reticulum, C-peptide stays in the Golgi secretory granules of beta cells in the pancreas and is co-secreted with insulin in response to glucose stimulation (Steiner et al. 1967). C-peptide has a central glycine-rich region which allows an appropriate arrangement of the A and B chains for insulin to form its disulfide bounds and achieve its tertiary structure. Although the amino acid sequences of the C-peptide from different species are quite variable, they do present several relatively well conserved sequences, such as the N-terminal acidic region, the glycine-rich central segment, and the highly conserved C-terminal pentapeptide. It has been demonstrated that mutations in the N-terminal region have significant effects on the in vitro refolding of proinsulin due to interactions with the A and B chains. C-peptide has an intramolecular chaperone like function important for proinsulin folding (Chen et al. 2002). On the other hand, C-terminal pentapeptide of C-peptide has been observed to obtain the full activity of intact C-peptide in stimulating Na^+/K^+-ATPase (Ohtomo et al. 1998) as well as increasing intracellular Ca^{2+} phosphorylation of mitogen-activated protein kinases in human renal tubular cells. The pentapeptide is capable of fully displacing C-peptide bound to renal tubular cell membranes (Ohtomo et al. 1998; Johansson et al. 2002; Pramanik et al. 2001). Being released into the bloodstream insulin is consumed very fast by the liver. Fast excretion and fast elimination results in a fluctuation of insulin concentration in blood. C-peptide is eliminated by the kidneys and this process is not as fast as insulin elimination. Insulin in blood is less stable than C-peptide. As a result, the half life of insulin in blood is significantly shorter (ca. 4 min) than that of C-peptide (ca. 33 min). The physiological serum concentration of C-peptide is in range from 0.3 to 1.1 nM. (Horwitz et al. 1975). It has been accepted that any hormone with specific cellular effects has a specific receptor at the cell surface, that it binds in a saturable and reversible manner and that it activates specific cellular events.

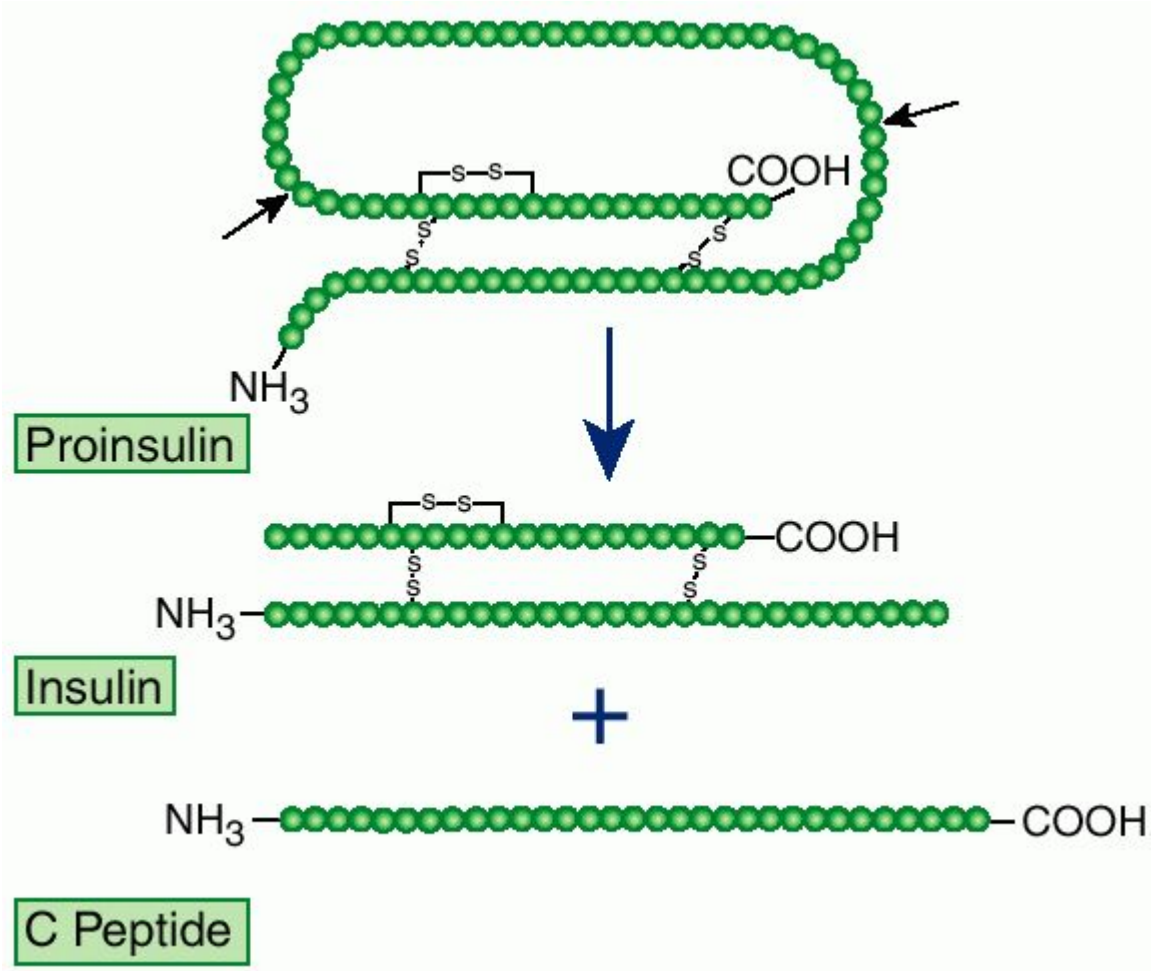

Figure 3. C-peptide synthesis within the endoplasmatic reticulum in β-pancreatic cells.

In early studies it was explained that the effects of C-peptide on diabetic vascular and neural dysfunction were mediated by nonchiral interactions instead of stereo-specific receptors (Ido et al. 1997; Ohtomo et al. 1998). C-peptide binding has been studied by using fluorescence correlation spectroscopy. This study demonstrated a 'receptor like binding' on cultured renal tubular cells and saphenous vein endothelial cells. The binding was inhibited by pertussis toxin, suggesting that binding was in some way coupled to a G protein activation. Henriksson and colleagues were found that C-peptide bind to the cell membranes of intact fibroblast giving the full saturation at 0.9 nM close to the physiological C-peptide plasma concentration (Henriksson et al. 2001). Rigler and colleagues described a stereo-

specific binding of C-peptide to a cell surface receptor. There was no cross reactions observed with insulin, insulin-like growth factor IGF-I, IGF-II or proinsulin (Rigler et al. 1999). Furthermore, COOH-terminal pentapeptide segment is essential for binding and represents an active site of the peptide (Ohtomo 1998) like in other biologically active peptides such as gastrin and cholecystokinin (Mutt et al. 1968).

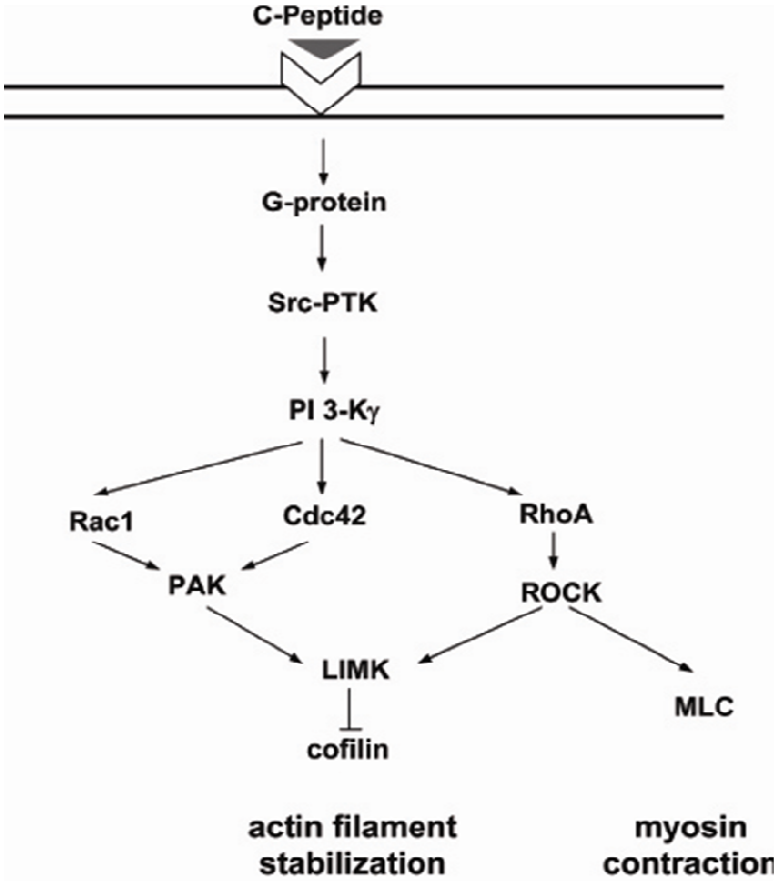

Figure 4. C-peptide-induced signalling pathways in CD4-positive lymphocytes (Aleksic 2009).

1.6. C-peptide and atherogenesis

1.6.1. C-peptide deposition in the vessel wall in early atherosclerosis

Patients with metabolic syndrome or type 2 diabetes mellitus exhibit an increased propensity for the development of a scattered and extensive pattern of arteriosclerosis (Beckman 2002). These insulin resistant patients demonstrate increased serum levels of insulin and C-peptide. During the last few decades, the role of insulin in atherogenesis has been examined by various groups and it has been suggested that insulin may promote lesion development, for example, by inducing proliferation of vascular SMCs (Trovati and Anfossi 2002). Other groups demonstrated that insulin exhibits anti-inflammatory and antiatherogenic properties in monocytes (Dandona et al. 2006; Dandona et al. 2007). In general, the role of insulin in atherogenesis stays unclear. For example, clinical and epidemiologic evidence is required to show that insulin may have harmful effects with respect to macrovascular events. For a long time, C-peptide has been considered to be biologically inert, but recent data suggest that C-peptide binds to specific yet unidentified cell surface receptors (Ohtomo 1998; Rigler et al. 1999; Henriksson et al. 2001). Marx and colleagues hypothesized that C-peptide might deposit in the vessel wall in these patients in early atherogenesis (Marx 2004). Immunohistochemical analyses of early arteriosclerotic lesions of patients with diabetes from the PDAY study revealed that C-peptide deposition takes place mainly in the subendothelial space and the intima. Some of the examined diabetic patients also exhibited a C-peptide deposition in the media. In contrast to this, only very little C-peptide deposition has been found in early arteriosclerotic lesions of non-diabetic subjects. Computer-assisted analyses revealed a significantly higher C-peptide deposition in lesions from diabetic individuals compared to lesions of non-diabetic subjects matched by age, sex and risk factors. In diabetic and non-diabetic subjects there was no positive staining for insulin.

1.6.2. C-peptide induces the migration of the inflammatory cells

Staining of parallel sections as well as immunofluorescence staining revealed a colocalization of C-peptide with monocyte/macrophages and CD4-positive lymphocytes in the intima in some of the diabetic individuals (Marx et al. 2004; Walcher et al. 2004).
In these studies C-peptide deposition has been found in 100% of the 21 diabetic individuals examined, while monocyte infiltration has been present in 77%, and CD4-positive lymphocyte infiltration only in 57% of all examined cases. In vitro migration assays, revealed that C-peptide induces the migration of both monocytes and CD4-positive lymphocytes. Interesting that insulin did not have such an effect. Stimulation of monocytes with C-peptide induced cell migration in a concentration dependent manner. The extent of C-peptide induced monocyte migration resembled the effect of the established monocyte chemokine MCP-1. The extent of C-peptide induced CD4-positive lymphocyte migration was similar to the effect of on T-cell chemokine RANTES. Combined stimulation of CD4-positive lymphocytes with C-peptide and RANTES did not have an additive migratory effect suggesting that they might use similar signalling pathways. In addition, C-peptide did not induce the migration of human neutrophils — cells not present in arteriosclerotic lesions. This underlines the specificity of C-peptide's chemotactic effects on monocytes and lymphocytes. Nevertheless, no migratory effect of C-peptide has been seen on B cells (Aleksic et al. 2009). All these data suggested that C-peptide deposition may lead to monocyte and CD4-lymphocyte migration into the vessel wall

1.6.3. C-peptide activates intracellular signalling pathways

Previous studies showed that C-peptide binds to a cell membrane and mediates its chemotactic activity through an unidentified pertussis toxin-sensitive G-protein coupled receptor, with subsequent downstream activation of PI3-kinase γ. Work from other groups has shown that Src-kinase is involved in interferon-gamma inducible protein-10 (IP-10) mediated chemotactic response of lymphocytes (Kuk-

htina 2005). C-peptide signalling includes the activation of pertussis toxin sensitive G-protein coupled receptor which activates Ca^{2+} dependent intracellular signalling. Aleksic and colleagues demonstrated that the migratory effect of C-peptide on CD4 positive lymphocytes was mediated by pertussis toxin sensitive G-proteins and PI-3 kinase gamma. The subsequent activation leads to an activation of Rho GTPases. Rho GTPases Rac1 and Cdc42 act via PAKs to stimulate LIMK, which phosphorylates and inhibits cofilin. This process allows increased accumulation of polymerized actin at the leading edge of cells. And RhoA stimulates MLC phosphorylation via ROCK activation which is important for cell body contraction and migration (Figure 4) (Aleksic et al 2009).

1.6.4. C-peptide induces proliferation of vascular smooth muscle cells

Vascular smooth muscle cells play an important role in the development of arteriosclerotic plaques by proliferating and then moving from the media into early lesions and fatty streaks (Ross 1999). Several mechanisms like platelet-derived growth factor (PDGF) released from activated platelets, secretion of cytokines, and growth factors from inflammatory cells have all been shown to induce VSMC proliferation during atherogenesis. Since C-peptide also colocalizes with SMCs in the media of early arteriosclerotic lesions in some diabetic subjects, it has been suggested that C-peptide could also exhibit biological activity in these cells (Marx 2003). Previous data have shown that C-peptide stimulation induced vascular smooth muscle cell proliferation via phosphorylation of Src and activation of PI-3 kinase and ERK1/2, suggesting that these signalling molecules are involved in C-peptide induced VSMC proliferation (Walcher 2006).

1.7. Aim of the study

The objective of this study was to investigate in an animal model the effects of C-peptide on the development of the atherosclerotic lesions.

2. Materials and Methods

2.1. Instruments

Instrument:	**Company:**
Centrifuge-mini	Eppendorf (Hamburg, Germany)
Cover glass	Menzel (Braunschweig, Germany)
Compress	Paul Hartmann, (Heidenheim, Germany)
Cryostat	Leica (Wetzlar, Germany)
Disposable hypodermic needle	Braun (Melsungen, Germany)
Incubator	Heraeus (Hanau, Germany)
Light microscope	Zeiss (Yena, Germany)
Microscope	Zeiss (Yena, Germany)
Microperfuser	Dispomed (Gelnhausen, Germany)
Multipette	Eppendorf (Austria)
Pipettes	Gilson (Middleton, Wi, USA)
Shaker	Branson (USA)
Scissors - fine	Fine Science Tools, (Heidelberg)
Stainless steel pins	Fine Science Tools, (Heidelberg)
Syringe	Becton Dickinson (Heidelberg, Germany)
Tweezers, fine	Fine Science Tools, (Heidelberg)
Tweezers, coarse	Fine Science Tools, (Heidelberg)
Vacuum Desiccator	Bel-Art Products (Jersey USA)
Weight	Sartorius (Gottingen, Germany)

2.2. Reagents

Product:	**Company:**
AB Complex	Vector Laboratories (Peterborough, United Kingdom)
Acetic acid	Sigma – ALDRICH (Steinheim, Germany)
3-amino-9-ethylcarbazole	Sigma – ALDRICH (Steinheim, Germany)
Acetone	Sigma – ALDRICH (Steinheim, Germany)
C-peptide rat (peptide)	New England Peptide (USA)
Formaldehyde	Sigma – ALDRICH (Steinheim, Germany)
Haematoxylin	Sigma – ALDRICH (Steinheim, Germany)
Heparin	Braun (Melsungen, Germany)
Hydrochloric acid	MERCK (Darmstadt, Germany
Insulin Elisa Kit	Millipore (Massachusetts, USA)
Kaisers glycerol gelatine	MERCK (Darmstadt, Germany)
H_2O_2 - 30%	Otto Fischer
Methanol	Sigma – ALDRICH (Steinheim, Germany)
2, Methyl-2-butanol 99%	Sigma –ALDRICH (Steinheim, Germany)
N' N'- dimethylformamide	Sigma – ALDRICH (Steinheim, Germany)
Oil-red-O	Sigma – ALDRICH (Steinheim, Germany
PBS Dulbecco's	PAA (Pasching, Austria)
Propylene-glycol	Sigma-ALDRICH (Steinheim, Germany)
Picric acid 1.2%	Sigma-ALDRICH (Steinheim, Germany)
RIA Kit	Linco Research (Missouri, USA)
Silicone elastomere	Factor II (Lakeside, USA)
Silicon elastomere, black	Factor II (Lakeside, USA
Sirius Red	Polysciences (Eppelheim, Germany)
Sodium chloride	Braun (Melsungen, Germany)
Surgical disposable Scalpels	Aesculap, Tuttlingen, Germany)

2,2,2 – Tribromoethanol 97%	Sigma-ALDRICH (Steinheim, Germany)
Tissue freezing medium	Lieca Mycrosystems (Nussloch, Germany)
Xylazin 2%	Alvetra (Heumuenster, Germany)

2.3. Mice and food

Male mice B6.129P2-*Apoe*^{tm1Unc}	Charles River Laboratories (Wilmington, USA)
High fat diet (E 15749-34)	SSNIFF (Soest, Germany)

2.4. Antibodies and buffers

Antibodies against:	Host	Dilution	Application	Product nr.	Company
C-peptide	Goat	1:25	Immunohistochemistry	4023-01	Linco
Mac-3	Rat	1:50	Immunohistochemistry	553322	BD Pharmigen
α-actin	Goat	1:75	Immunohistochemistry	sc-1616	Santa Cruz

0,1 M Acetat buffer

0.1N Acetic acid

0,1 N Sodium acetat

PBS pH 7.4

8 g Sodium chloride NaCL

0.2 g Potassium chloride KCL

0.27 g Potassium dihydrogen phosphate KH_2PO_4

1,44 g Disodium hydrogen phosphate Na_2HPO_4 x $2H_2O$

2.5. Immunohistochemistry

2.5.1. Avidin-Biotin method

Serial cryostat sections (5 µm) have been stained after the standard Avidin-Biotin-Complex (ABC) procedure. Frozen sections have been air dried, immersed in PBS due to rehydration. Eliminating endogenous peroxidise activity has been performed by pretreatment of the tissue sections with 0.3% hydrogen-peroxidase activity before the incubation of the primary antibody. Non specific background staining is non immunological binding of the specific immune sera by hydrophobic and electrostatic forces to definite sites within the tissue section. This form of background staining is usually uniform and can be reduced by blocking those sites with normal serum. Therefore all sections have been pretreated 30 min with 50µL of normal serum according to the first antibody. Incubation with different dilutions of antibodies have been preformed for 45 min at 37 °C. The unlabeled primary antibody reacts with tissue antigen. After incubation all slides have been washed with PBS to remove residual antibody. The secondary antibody reacts with different antigenic sites on the primary antibody. The secondary antibody has to be against IgG of the animal species in which the primary antibody has been raised. Slides were incubated for 30 min at 37°C with secondary antibody. This antibody is biotinilated. Biotin is a low molecular weight vitamin and has very strong affinity for protein avidin. After this step all slides have been washed in PBS to remove residual antibody. Typically, avidin and biotinilated enzyme (peroxidise) are mixed together at room temperature to form the complex. An aliquot of this solution (50 µL) has been added to the tissue and any remaining biotin binding sites on the avidin bind to the biotinilated antibody that has been already bound to the tissue. This step is also incubated at 37°C. The result is a greater concentration of enzyme (three enzyme molecules to one avidin molecule) at the antigenic site and therefore an increase in signal intensity and sensitivity. The peroxidise has been developed by the AEC substrate and the red colorimetric end products has been received. Nuclei have

been stained with haematoxylin - eosin solution for three min, washed in tap water for ten min and mounted in Kaiser's gelatine.

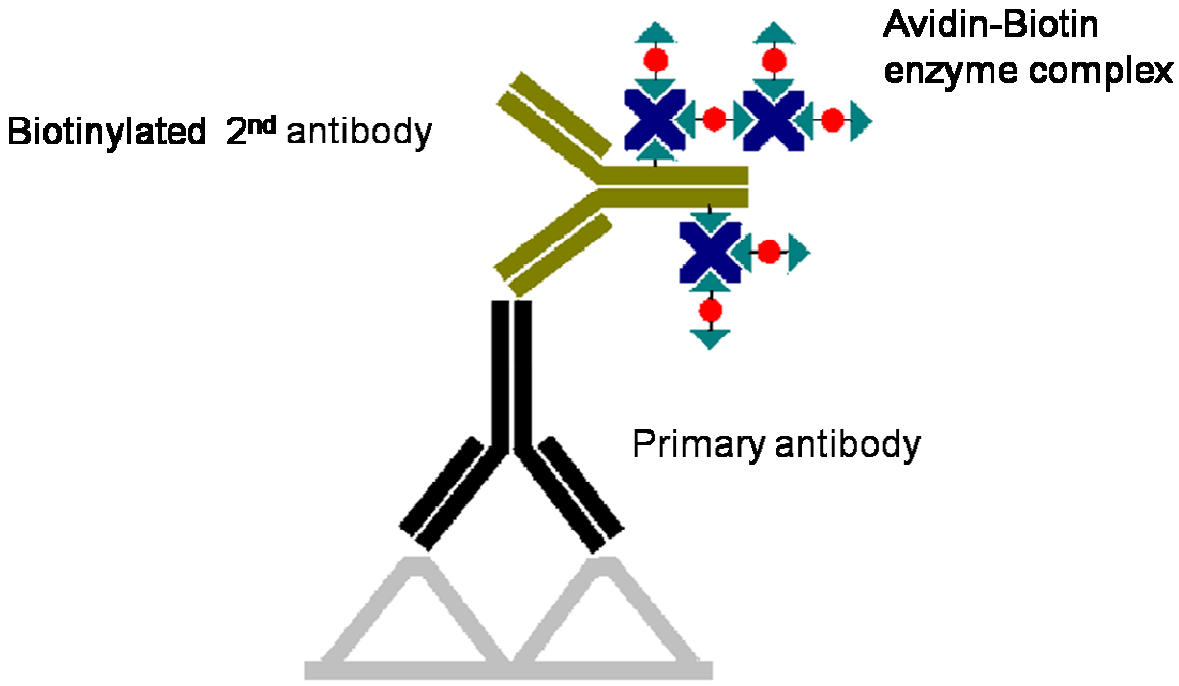

Figure 5. Schematic illustration of antibody binding in Avidin-Biotin method.

2.5.2. Oil-red-O staining for lipids

Deposition of lipids in en face preparations of thoracic and abdominal aortas have been determined by an Oil-red-O staining. After euthanizing an animal, aortas have been fixed in 4% paraformaldehyde, subsequently, washed for two min in 100% propylene-glycol solution, then stained with Oil-red-O solution for three hours at the room temperature. After that, the slides have been washed four times in 85% propylene-glycol solution. Subsequently, the aortas have been opened longitudinally to the aortic bifurcation, pinned on the surface of the black wax with 0.2-mm steel pins.

Fresh frozen tissue has been cut in 5 µm thick sections and mount on the slides. They have been fixed in 4% formaldehyde solution for ten min. Slides have been air dried for 30 to 60 min, than rinsed in distilled water. The slides have been placed in an absolute propylene glycol for two to five min to avoid carrying water into the Oil-red-O solution. Next, slides were stained in pre-warmed Oil-red-O solution for 20 min in a 60°C incubator. Further, the slides have been placed in 85% propylene-glycol solution for two to five minutes and subsequently have been rinsed in two changes in distilled water. Nuclei were stained in haematoxylin for 30 seconds. The slides have been washed thoroughly in running tap water for ten minutes and at the end mounted in Kaiser's gelatine.

2.5.3. Picrosirius red staining for collagen

Collagens type I and III were stained by Picrosirius red solution. Frozen tissue sections were incubated for 90 min in 0.1% Picrosirius red powder dissolved in saturated picric acid. After rinsing twice in 0.01 M HCL, and in distilled water, sections have been dehydrated for a short time with 70% ethanol and mounted. Slides stained with Picrosirius red have been analyzed by polarized light.

2.6. Insulin Elisa assay

This assay is a sandwich Elisa and it is based on capturing of insulin molecules from samples to the wells of a microtiter plate coated with monoclonal mouse anti-rat insulin antibodies and the binding of biotinylated polyclonal antibodies to the captured insulin. The stripes were collected in an empty plate holder and washed each well three times with 300 µL of diluted TBS wash buffer per wash. The wash buffer has been decanted to remove the residual amount from all wells by inverting the plate and tapping onto absorbent towels. Furthermore, 10 µL assay buffer was added to the blank and to the each of the sample wells.

After that, 10 µL matrix solution was added to the blank, standard and control wells. Standards and controls were added in order to descending concentration to the wells. 10 µL samples in duplicates and 80 µL detection antibody were added to all wells. The plate was covered with the plate sealer and incubated at room temperature for two hours on a orbital microtiter plate shaker set at moderate speed of about 400 to 500 rpm.

Furthermore, the wells have been washed three times with diluted wash buffer, 300 µL per well, to wash away all unbound materials from the samples. Then 100 µL of enzyme solution has been added to each well, namely-binding the horseradish peroxidise to the immobilized biotinylated antibodies. The plate was covered with sealer and incubate with moderate shaking at room temperature for 30 min. In the next step, free enzyme conjugates were washed away. The wells were washed six times with diluted wash buffer. After that, 100 µL of substrate solution were added to each well. After approximately 15 min blue colour has been formed. In the last step 100 µL of stop solution has been added when the blue colour turned into yellow after acidification. In this step a quantification of immobilized antibody-enzyme conjugates has been preformed by monitoring horseradish peroxidise activities in the presence of the substrate 3,3' ,5, 5'-tetramethylbenzidine. The enzyme activity has been measured spectrophotometrically by the increased absorbency at 450 nm.

2.7. C-peptide radioimmunoassay – RIA

Rat C-peptide radioimmunoassay kit has been used to measure C-peptide levels in mouse serum because of the high sensitivity of this technique. On the first day performing this assay, identical volumes of blood serum samples have been mixed with rat-C-peptide antibody and incubated over night at 4 °C. On the second day, ^{125}I-Rat C-peptide tracer has been added and incubated with constant dilution of serum. The concentration of antigen binding sites on the antibody is limited. There is a competition between labelled tracer und unlabeled antigen for the limited and constant number of binding sites on the antibody. The amount of tracer bound to the antibody will decrease as the concen-

tration of unlabeled antigen increases. On the third day a precipitating reagent has been added to all tubes to precipitate free tracer. A pellet has been formed after centrifugation. The supernatant was decanted immediately after centrifugation and the pellet was count in a gamma counter for 1 minute.

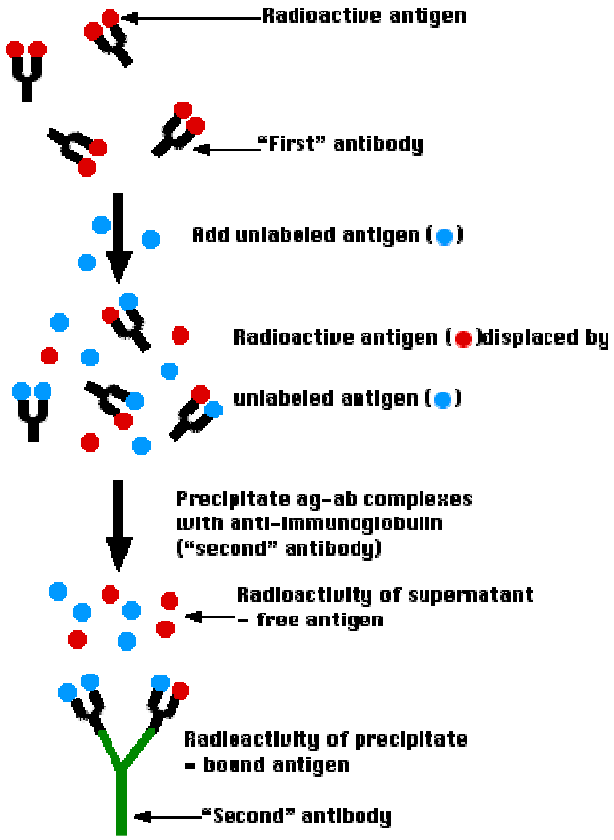

Figure 6. Schematic illustration of antibody binding in radioimmunoassay.

2.8. Mice treatment

2.8.1. Study design

In our experimental model we used ApoE-deficient mice with C57BL/6 background. ApoE-deficient male mice were obtained from the Charles River Laboratories. The mice were housed individually with food and water provided *ad libitum.* This study included four experimental groups:

1) **Control group 1** - Standard chow diet (n=5);
2) **Control group 2** - High fat diet (n=8);
3) **Placebo group** - High fat diet + distilled water (n=17);
4) **C-peptide group** - High fat diet + C-peptide (n=18).

At the beginning of the experiment blood was obtained from the tail vein from each mouse to determine basal C-peptide levels in serum in each group. After that, control group 1 was fed with a standard chow diet until the end of the study. The three other groups were fed with a high fat diet for a week. Subsequently, all groups started with the treatment or were used as a controls. The mice in the second, control group 2 were just on the high fat diet for the next twelve weeks. The mice in the third, placebo group were on the high fat diet treated with distilled water for the next twelve weeks. And the mice in the fourth, C-peptide group were on the high fat diet simultaneously injected with 200 nMol of dissolved C-peptide two times daily for the next twelve weeks. After twelve weeks of treatment blood was drawn again (four hours after last injection in the treated groups), to determine serum C-peptide levels after the treatment. On the next day the animals have been euthanized (Figure 7).

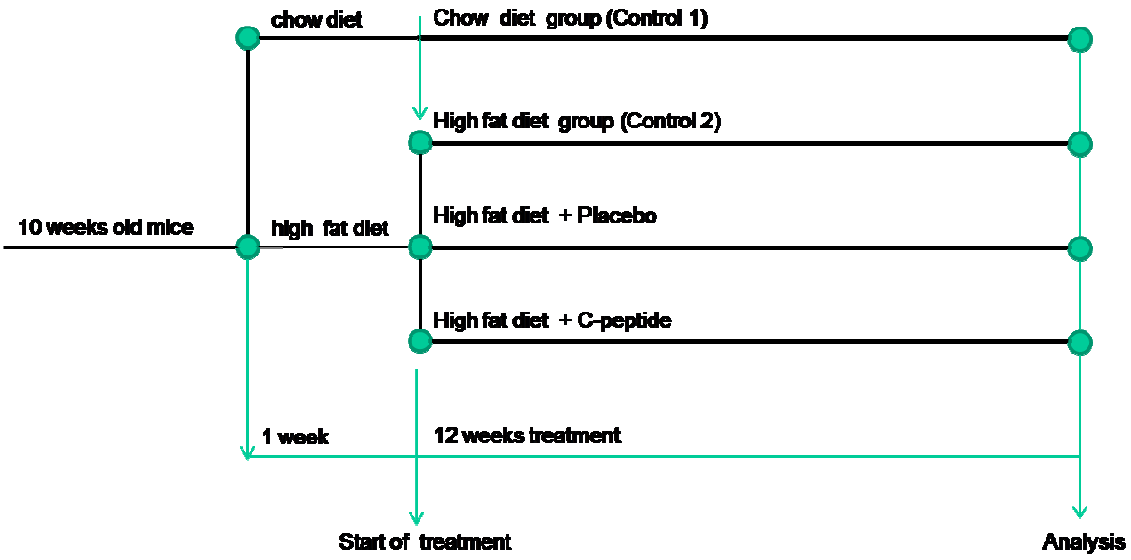

Figure 7. Study design

2.8.2. Preparation procedure

The mice have been anesthetized by an intraperitoneal injection 2, methyl-2-butanol (delivered from 1 mL syringe with 30G needle). Before that, an intraperitonel injection of heparin was given. The depth of anaesthesia was tested by lack of response to a certain squeeze to a hind foot. Additional anaesthesia was administrated in 50 µL increments until this depth has been achieved. The age of the mice has been kept constant ± 0.5 weeks, since lesion development is age dependent (Veillard 2004). Additionally, the weight of mice was determined. The ventral surface of the mouse was wetted with water or 70% ethanol to keep the hair matted down. The skin has been cut from the abdomen to the top of the thorax. After that, the abdominal wall bellow the ribcage was opened. The sternum has been lifted with tweezers and the diaphragm cut. Then, the lower part of ribcage has been cut away to partially expose the heart. Blood was drawn from the heart by sticking the needle of 1mL syringe into the apex of the left ventricle. Blood was drawn by pulling the plunger and slowly twisting the needle and collected into a tube. The mouse has been euthanized at the point of ex-

sanguinations. After centrifugation the serum was transferred into a fresh tube. The residual ventral part of the ribcage was removed and using micro dissection scissors all the fat and tissue surrounding the heart including the pulmonary artery and veins were cut. Heart and aorta were cleaned from fat and connective tissue, through the descending arterial tree along until iliac bifurcation has been reached. Briefly, mice hearts were perfused at physiological pressure with normal saline via the left ventricle, and the hearts and aortas were removed en bloc. The aorta was stored in 4% paraformaldehyd (at 4°C). The heart and aortic arch were frozen in tissue freezing medium and stored at -80 °C.

2.8.3. Blood profile

Heparinized blood samples were centrifuged at 3600 rpm for 10 min. The serum was removed to 1.5 ml tubes and stored at -80°C. Serum total cholesterol, HDL, LDL cholesterol and triglycerides have been measured in the Clinical Chemistry Laboratory. Insulin levels from mouse serum were determined following manufacturer method for Insulin Elisa kit. Glucose levels were determined from mouse serum using standard glucose stripes.

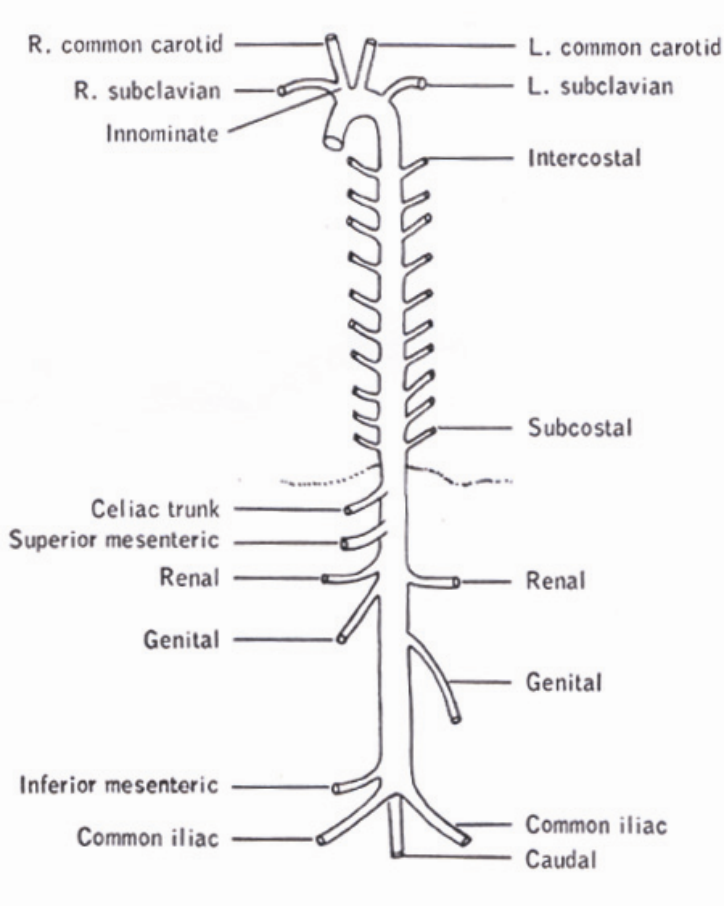

Figure 8. Drawing of the main artery branching in mouse circulatory system (Green 2007; Biology of the laboratory mouse)

2.9. Analysis

2.9.1. Tissue analysis

To quantify the extent of atherosclerotic lesions, the longitudinally sections of the aortic arch, cross-sections of aortic root as well as longitudinally opened abdominal aortas were analyzed microscopically in all mice. Mouse atherosclerotic lesions have been analyzed in longitudinal sections from a segment of the lower curvature of the aortic arch (defined using a perpendicular line dropped from the right side of the innominate artery and from the left side of the left sub-

clavian artery (Figure 9 A). Inside the aortic root, lesion areas were analyzed in cross-sections obtained at the level of all three leaflets of the aortic valve (Figure 9 B). The percentage of area stained for C-peptide, macrophages, lipids, smooth muscle cells or collagen have been determined via computer-assisted image quantification (ImageProPlus Software). Atherosclerotic lesion burden was quantified along the luminal surface of the aorta. Descending aorta (thoracic and abdominal) has been stained with Oil-red-O solution, placed on the black wax and opened longitudinally. The atherosclerotic plaque area was expressed as a percentage of the total luminal surface area of the aorta.

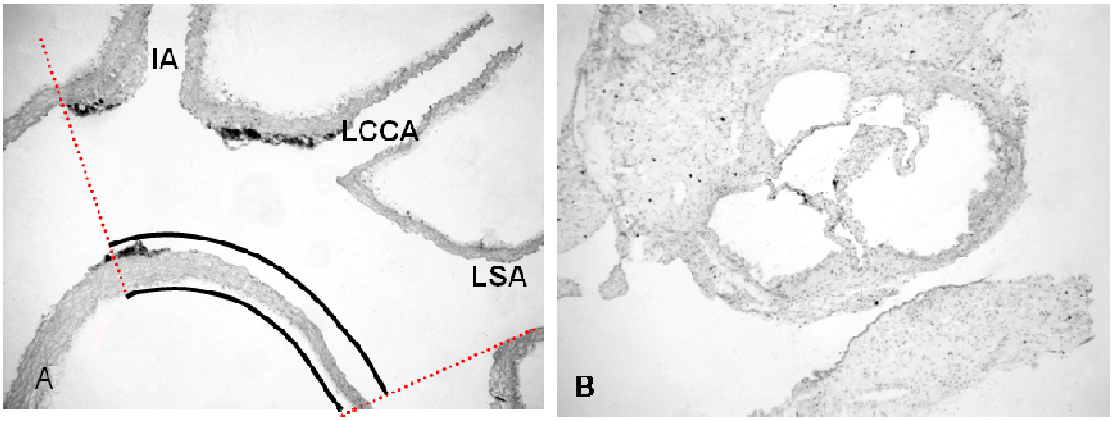

Figure 9. A) Representative photomicrograph of a mouse aortic arch longitudinal section, used for the analysis of a total wall area by computer-assisted image quantification. (IA indicates *inominate artery*, LCCA, *left common carotid artery*, LSA, *left subclavian artery*). **B)** Representative photomicrograph of a mouse aortic root cross section at the level of all three leaflets of the aortic valve.

2.9.2. Statistical analysis

All data are expressed as arithmetic mean ± standard error of mean (SEM). n values refer to the number of mice in each experimental group. Differences were analyzed by unpaired Student t - test with P value of <0.05 considered as significant.

3. Results

3.1. C-peptide and blood profile

To test the hypothesis that C-peptide has a role in atherosclerosis, increased levels of C-peptide has been established in an animal model. ApoE deficient mice were divided into four experimental groups. Mice in the control group 1 were on the chow diet, whereas those in the control group 2 on the high fat diet. The placebo group mice were on the high fat diet simultaneously treated with water. C-peptide group mice were on the high fat diet simultaneously treated with C-peptide. Serum C-peptide levels at the beginning of the study were in the physiological range. Furthermore, basal C-peptide levels in the placebo and C-peptide group did not differ (1.7 ± 0.2 nmol/L vs. 1.4 ± 0.2 nmol/L) (Figure 10). Peptide levels in the treated groups after twelve weeks of treatment were elevated. The C-peptide treated group exhibited fivefold induction in serum levels compared with levels of C-peptide in the placebo group after treatment (placebo vs. C-peptide; 2.6 ± 0.7 nmol/L vs. 12.8 ± 1.8 nmol/L, *P<0.05) (Figure 10).

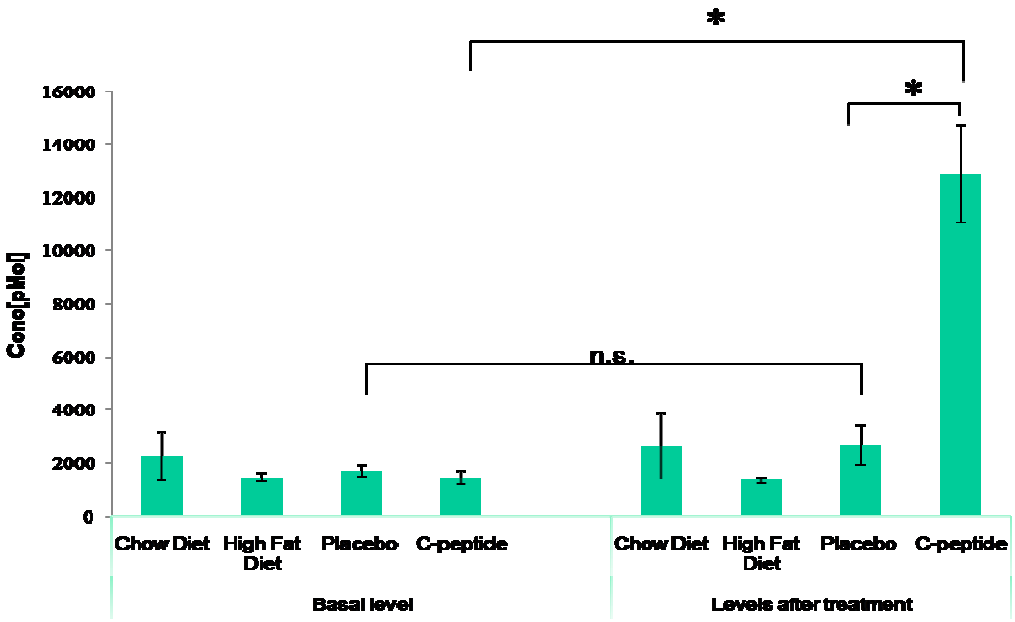

Figure 10. Subcutaneous application (200nM) of C-peptide increases serum levels of C-peptide. C-peptide levels in mouse serum at the beginning and after twelve weeks of treatment.

C-peptide levels were measured with RIA in blood samples taken 4 hours after the last application of dissolved peptide (chow diet n=5; high fat diet n=6; placebo n=17; C-peptide n=18), n.s.- not significant; *P<0.05

To gain further insight into a blood profile of ApoE-deficient mice it has been investigated a critical feature of these mice (Javien et al. 2004), namely lipid levels in mouse serum. In all four groups total cholesterol, triglycerides, HDL and LDL levels were measured (Table 2). All mice revealed an elevated level of total cholesterol, however it did not differ between the two experimental groups (placebo vs. C-peptide; 11.87 ± 0.57 mmol/L vs. 13.46 ± 1.38 mmol/L) as well as the group of mice which were on the high fat diet (13.59 ± 1.2 mmol/L). As expected, the control mice on the chow diet demonstrated lower levels of total cholesterol (7.22 ± 0.59 mmol/L).

Next, glucose and insulin levels have been examined (Table 3) in these hypercholesterolemic mice. A subset of mice (n=8 per group) fasted six hours before blood was drawn. No difference in insulin levels between two experimental groups have been found (placebo vs. C-peptide; 0.49 ± 0.04 ng/mL vs. 0.41 ± 0.03 ng/mL, P=0.21). Moreover, there were no difference between the placebo and the C-peptide group in serum glucose levels (placebo vs. C-peptide; 356 ± 21.59 mg/dL vs. 280 ± 41.52 mg/dL, P=0.12). It should be noted, that glucose levels in both groups were slightly elevated, indicating that those mice might be insulin resistant.

Finally, the mice weight was compared. The results are shown in Table 4. The weight was similar in both experimental groups as well as in the control groups on the chow and high cholesterol diet, suggesting that high cholesterol treatment did not induce obesity in treated mice.

Table 2. Total cholesterol, triglycerides, HDL, LDL levels in mouse serum at the end of the treatment. Data represent mean ± SEM. (*P<0.05 for Control Group + Chow Diet vs. C-peptide Group + High Fat Diet), n values refer to the number of mice in each experimental group.

	Control Group 1 (Chow diet) (n=5)	Control Group 2 (High Fat diet) (n=8)	Placebo Group +High Fat diet (n=17)	C-peptide Group +High Fat diet (n=18)
Cholesterol (mmol/L)	7.22 ± 0.26*	13.59 ± 1.2	11.87 ± 0.57	13.47 ± 1.381
Trigliceride (mmol/L)	0.79 ± 0.1	0.69 ± 0.11	0.67 ± 0.06	0.85 ± 0.18
HDL (mmol/L)	0.52 ± 0.01*	0.32 ± 0.04	0.29 ± 0.01	0.33 ± 0.03
LDL (mmol/L)	2.48 ± 0.44*	7.93 ± 1	6.37 ± 0.46	7.05 ± 0.36

Table 3. Glucose and insulin levels in mouse serum at the end of the treatment. Differences between two groups are not statistically significant. Data represent mean ± SEM. n values refer to the number of mice in each experimental group.

	Placebo Group + High Fat Diet (n=8)	C-peptide Group + High Fat Diet (n=8)
Glucose (mg/dL)	356 ± 21.59	280 ± 41.52, P=0.12
Insulin (ng/mL)	0.49 ± 0.04	0.41 ± 0.03, P=0.21

Table 4. Mice weight at the end of the treatment. Differences between groups are not statistically significant. Data represent mean ± SEM. n values refer to the number of mice in each experimental group.

	Control Group 1 (Chow diet) (n=5)	Control Group 2 (High Fat diet) (n=8)	Placebo Group +High Fat diet (n=17)	C-peptide Group + High Fat diet (n=18)
Weight (g)	29.69 ± 0.48	31.49 ± 0.74	30.99 ± 0.72	30.75 ± 0.57

3.2. C-peptide deposition in early lesions of aortic arch

In the first set of experiments, C-peptide deposition in early atherosclerotic lesions have been examined in longitudinal sections of the aortic arch (Figure 9 A). Immunohistochemical analysis of the aortic arch showed prominent C-peptide staining in the C-peptide treated group with only scarce deposition in the placebo group. In the C-peptide treated group has been found a significantly higher extent of C-peptide positive areas (placebo vs. C-peptide; 0.83 ± 0.13% vs. 2.13 ± 0.41%, $P<0.05$) (Figure 11 C). Staining of sections with an isomatched IgG at similar concentration showed no immunoreactivity, thus affirming the specificity of the detected signals (Figure 11 B). To further verify the specificity, we stained for C-peptide in the control groups (Figure 11 A). These mice did not get a C-peptide treatment, one group was on the chow diet and a second group on high fat diet. The chow diet group showed rare or no staining for C-peptide (0.03 ± 0.03%) while high fat control group provide similar amount of C-peptide positive area as placebo (0.67 ± 0.28%). Figure 11 D represents a proportion of C-peptide positive area in all four experimental groups.

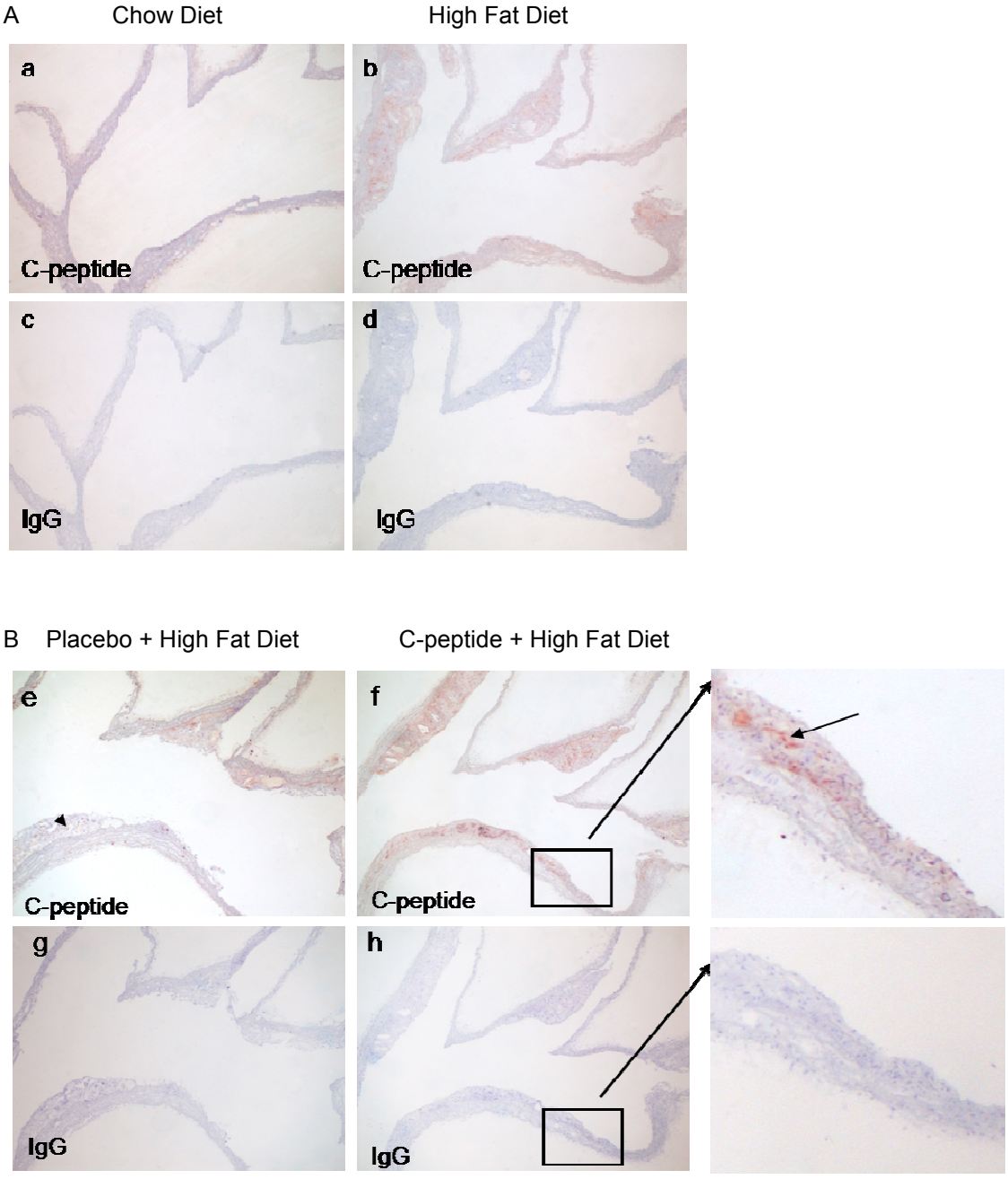

Figure 11. **A)** C-peptide deposition in the aortic arch. Representative longitudinal sections of aortic arch show C-peptide deposition in control mice on the chow diet (a) and mice on the high fat diet (b). Adjacent sections (c) and (d) stained with the identical amounts of type and class matched IgG show no immunoreactive C-peptide. **B)** Representative longitudinal sections of aortic arch show C-peptide deposition in atherosclerotic plaque in placebo (e) and C-peptide treated mice (f). Adjacent sections (g) and (h) stained with the identical amounts of type and class matched IgG show no immunoreactive for C-peptide. Arrow indicates C-peptide positive area.

C

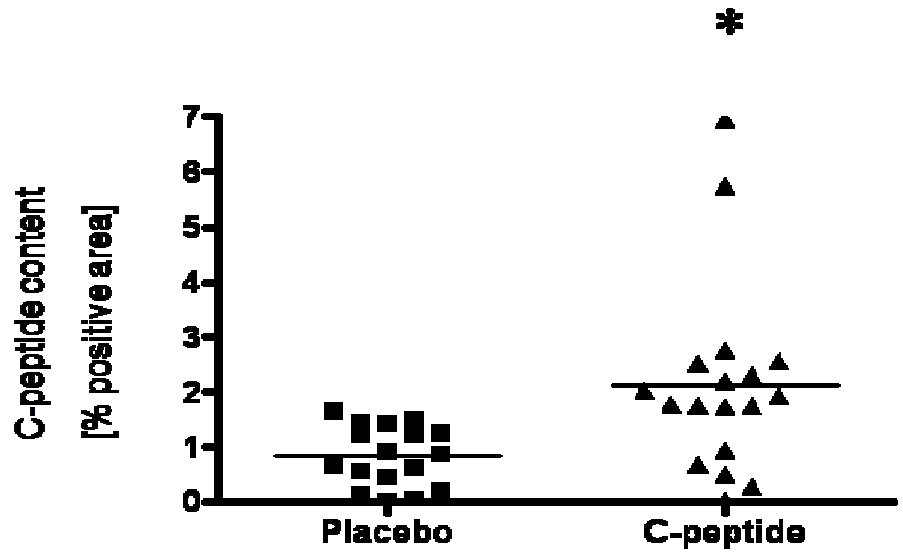

D

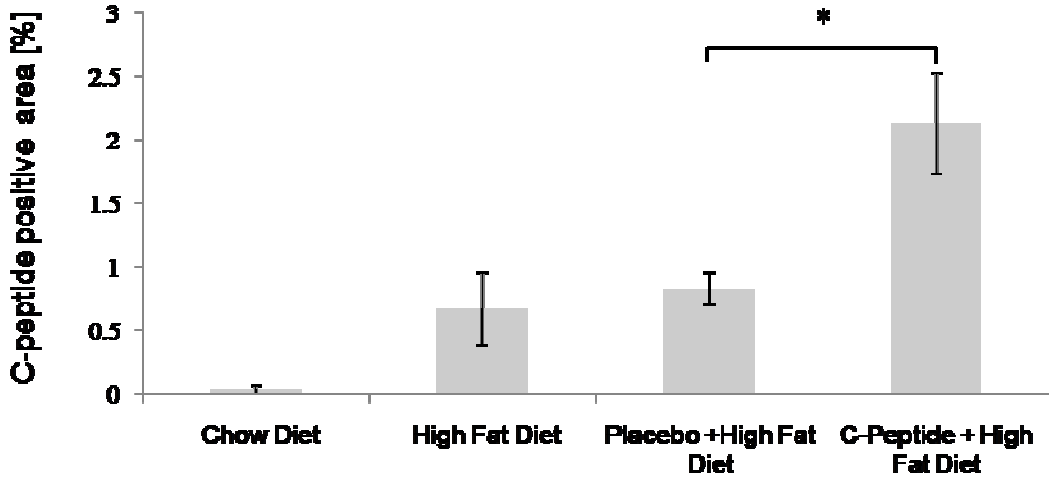

Figure 11. **C)** C-peptide deposition in the aortic arch. Analysis of C-peptide positive areas determinate via computer-assisted image quantification. Each data point represents a value from a single mouse. **D)** Diagram represents proportion of C-peptide positive areas in all four experimental groups, determined via computer-assisted image quantification (chow diet: n=5, high fat diet: n=8, placebo: n = 17, C-peptide: n = 18). Bars represent mean ± SEM *P<0.05

3.3. C-peptide increases inflammatory cell content in aortic arch

The monocyte/macrophages content have been analysed in atherosclerotic lesions in longitudinal sections of aortic arch in placebo and C-peptide group of mice after twelve weeks of C-peptide treatment (Figure 12 B). Furthermore, it has been compared with both control groups of mice, to determine whether subcutaneous injections as additional stress factor have an impact on monocyte/macrophages content in these mice (Figure 12 A). Computer-assisted analysis revealed that C-peptide treatment significantly increases monocyte/macrophages deposition in atherosclerotic lesions (placebo vs. C-peptide; 0.72 ± 0.16% vs. 1.61 ± 0.25%) (Figure 12 C). However, the chow diet control mice exhibited the minimal extent of monocyte/macrophages (0.16 ± 0.13%) as expected and the high cholesterol group of mice showed similar extent for Mac-3 positive area as the placebo mice (1 ± 0.2%) (Figure 12 D).

Next, parallel sections of the aortic arch have been stained with anti C-peptide antibody and Mac-3 antibody. Immunohistochemical staining of these sections showed possible colocalization of C-peptide with monocyte/macrophages in early atherosclerotic lesions in our experimental model (Figure 13).

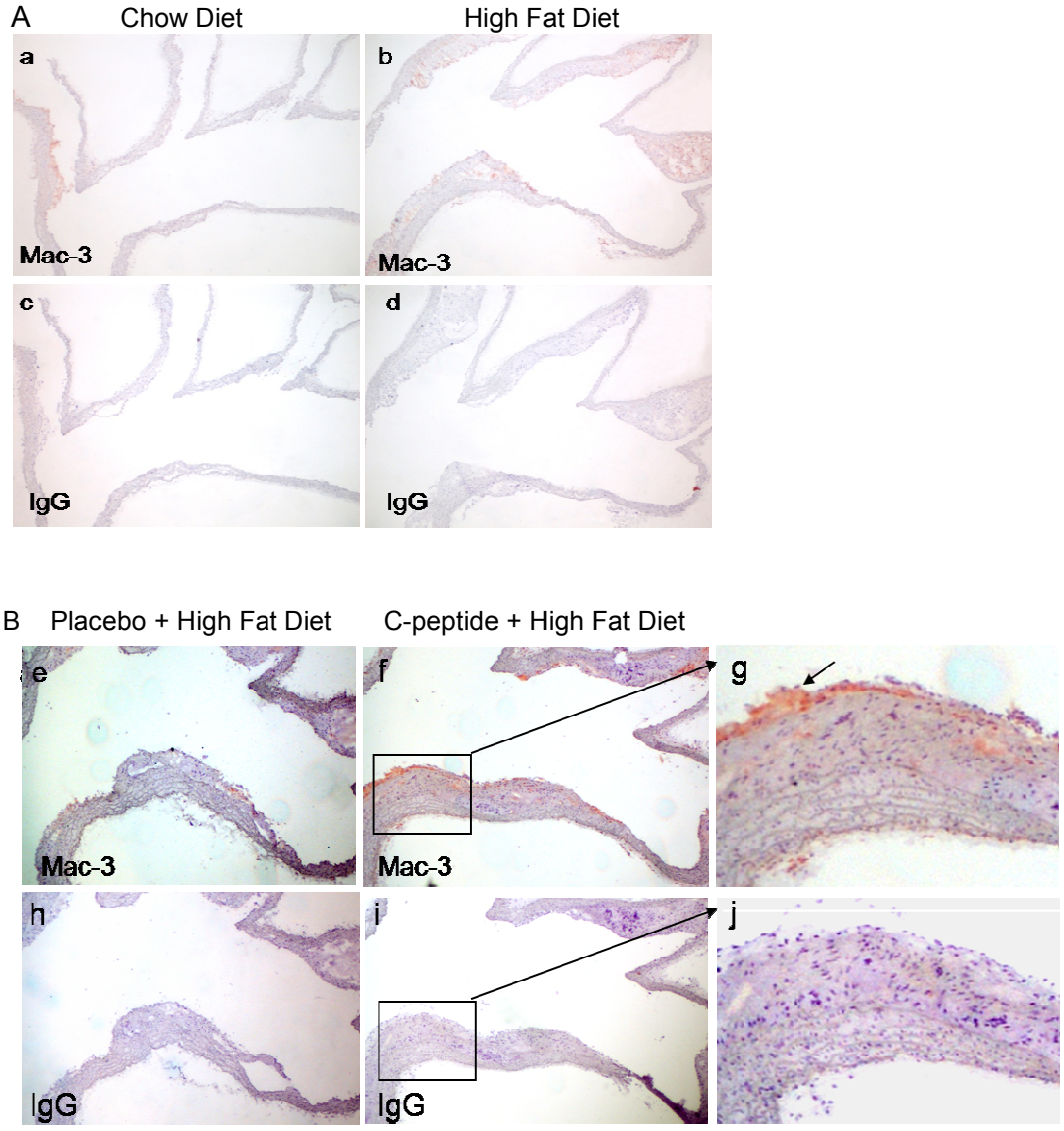

Figure 12. A) C-peptide treatment increases monocyte/macrophage content in the aortic arch. Representative images of longitudinal sections of mouse aortic arches stained for the expression of Mac-3, represent monocyte/macrophages in the chow diet control group (a), high cholesterol diet control group (b). (c), (d) represent IgG matching controls. Arrow indicates Mac-3 positive area (red). **B)** Placebo mice (e) showed little Mac-3 positive area compared with C-peptide treated mice (f). (h) and (i) represent IgG matching controls.

C

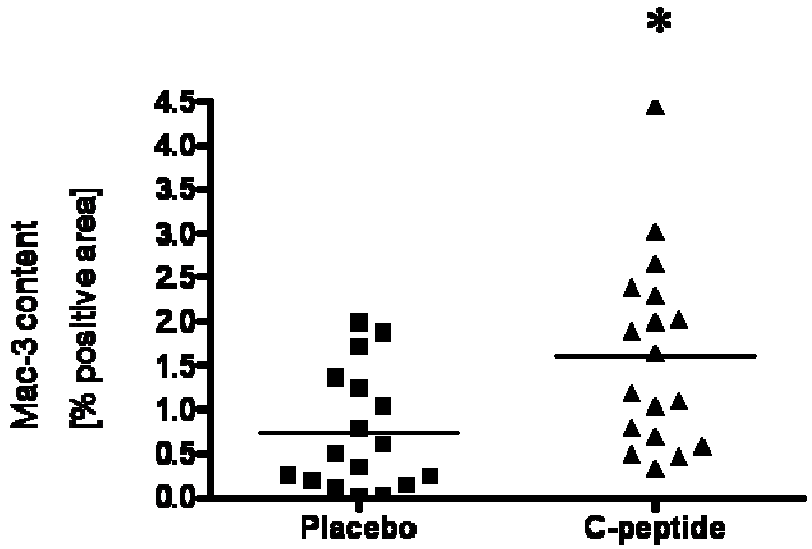

D

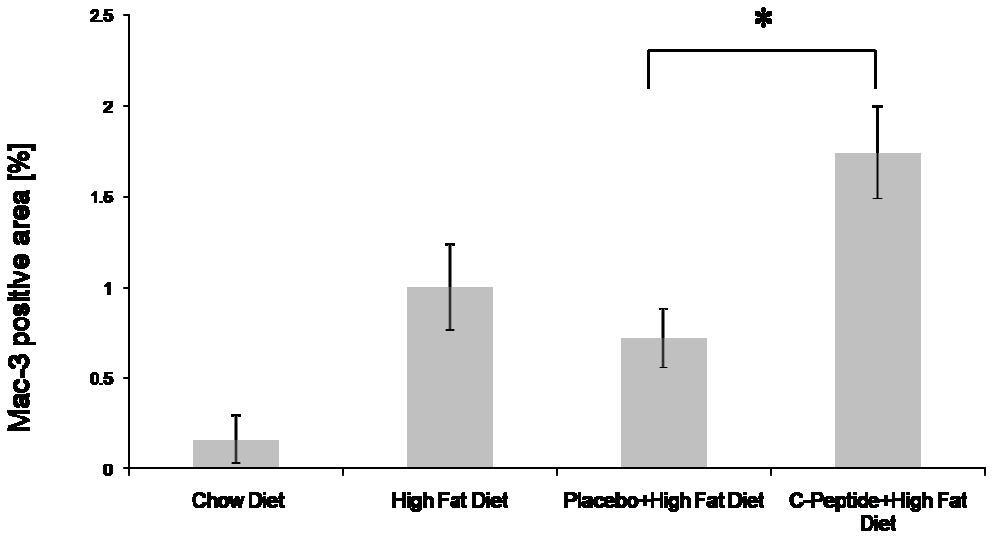

Figure 12. C) C-peptide treatment increases monocyte/macrophage content in the aortic arch. Analysis of Mac-3 positive areas determined via computer-assisted image quantification. Each data point represents a value from a single mouse. **D)** Diagram represents proportion of Mac-3 positive areas in four experimental groups (chow diet: n=5, high fat diet: n=8, placebo: n = 17, C-peptide: n = 18). Bars represent mean ± SEM.* P< 0.05

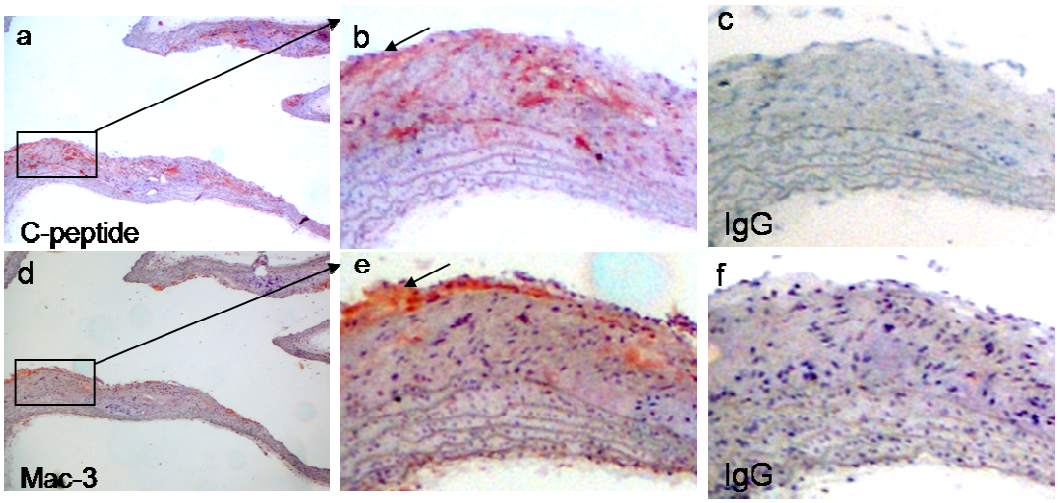

Figure 13. C-peptide colocalize in early atherosclerotic lesions with monocyte/macrophages in ApoE deficient mice. Representative mouse aortic arch demonstrates C-peptide staining in early lesion (a). High power view of this area is indicated by rectangle in a. Parallel section stained with Mac-3 antibody demonstrates monocyte/macrophages (d). High power view of this area is indicated by rectangle in d. Arrows indicate colocalization of C-peptide with monocyte/macrophages. (c), (f) represent IgG matching controls.

3.4. C-peptide increases smooth muscle cell content within aortic arch

The C-peptide effect on the content of smooth muscle cells in aortic arch has been investigated performing immunohistochemical staining for α-actin (Figure 14 A, B). Our data showed that treatment with C-peptide increases smooth muscle cell content within the aortic arch (placebo vs. C-peptide; 2.36 ± 0.34% vs. 4.79 ± 0.54%, $P<0.05$), while both control groups exhibited similar content of smooth muscle cells in range with placebo group (chow diet group vs. high cholesterol diet group; 2.01 ± 0.39% vs. 2.82 ± 0.5%) (Figure 14 B, C).

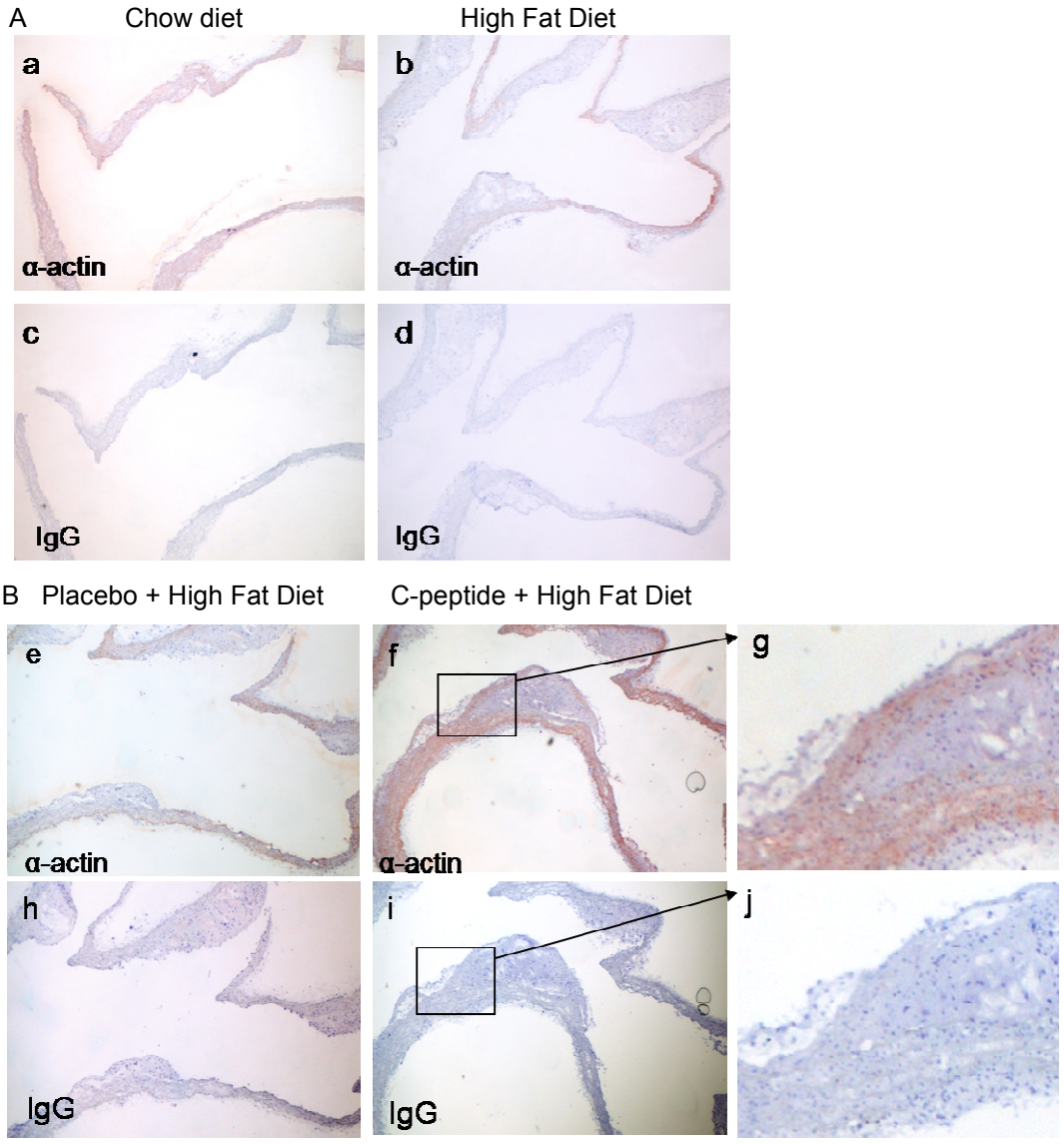

Figure 14. A) C-peptide treatment increases smooth muscle cell content within the aortic arch. Expression of α-actin positive area within aortic arch in chow diet control mice (a), high fat diet control mice (b). (c) and (d) represent IgG matching controls. **B)** Immunohistochemical staining for the expression of α-actin in aortic arch in C-peptide treated mice showed increased smooth muscle cell deposition (f) compared to placebo (e). (h) and (i) represent IgG matching controls.

C

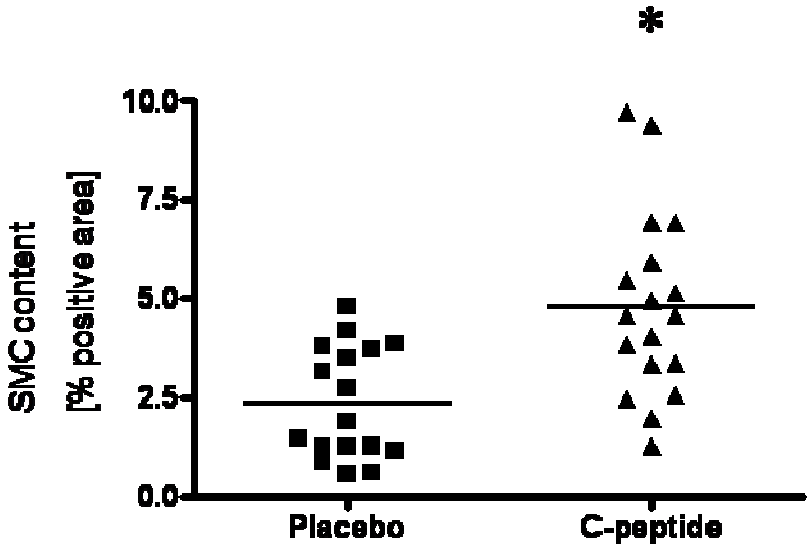

D

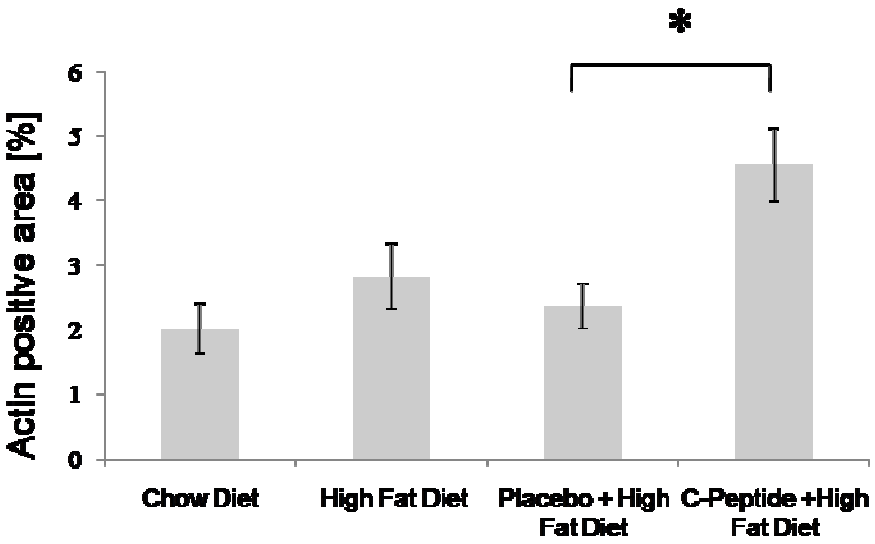

Figure 14. C) C-peptide treatment increases smooth muscle cell content within the aortic arch. Analysis of α-actin positive areas determined via computer-assisted image quantification. Each data point represents value from a single mouse. **D)** Diagram represents proportion of smooth muscle cell positive areas in all four experimental groups (chow diet: n=5, high fat diet: n=8, placebo: n = 17, C-peptide: n = 18). Bars represent mean ± SEM. *P < 0.05

3.5. C-peptide increases lipid content in mice

The quantification of aortic lesions is an important endpoint for evaluating atherosclerosis in the mouse model. A fast and simple method of lipid detection in mouse vessel is the staining with neutral lipid-targeting lysochrom Oil-red-O (Beattie et al. 2009). The treatment with C-peptide increases lipid content in aortic arch compared to the placebo mice (placebo vs. C-peptide; 9.51 ± 1.6% vs. 14,82 ± 1.5%) (Figure 15 A). Mice on the chow diet showed a small lipid deposition in the aortic wall (2.27 ± 0.9%). The control mice on the high fat diet showed similar lipid extent (8.45 ± 1.4%) as placebo mice (Figure 15 B, C).

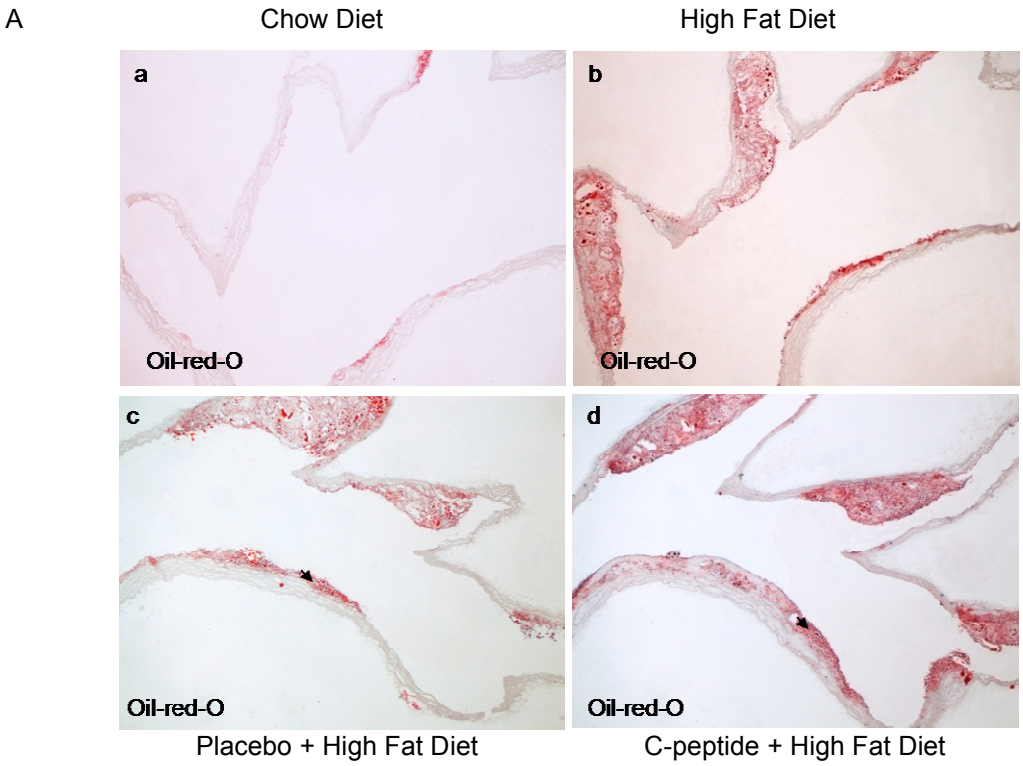

B

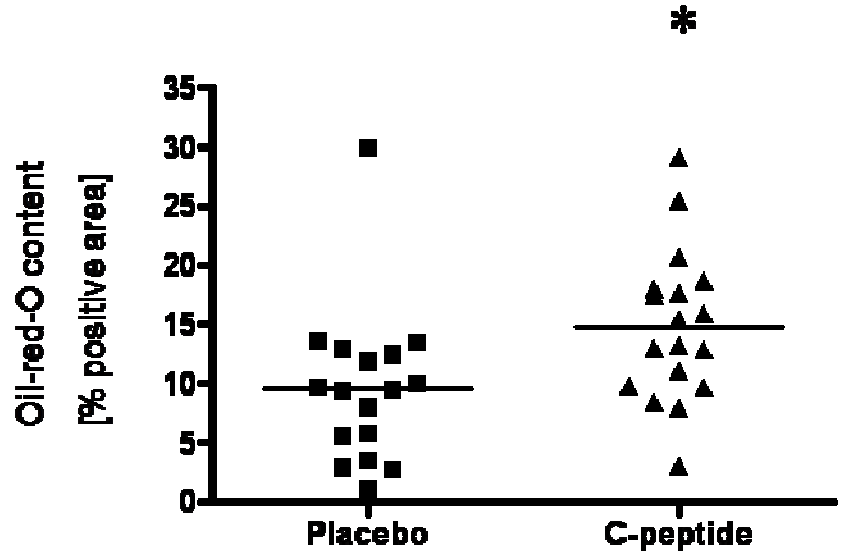

C

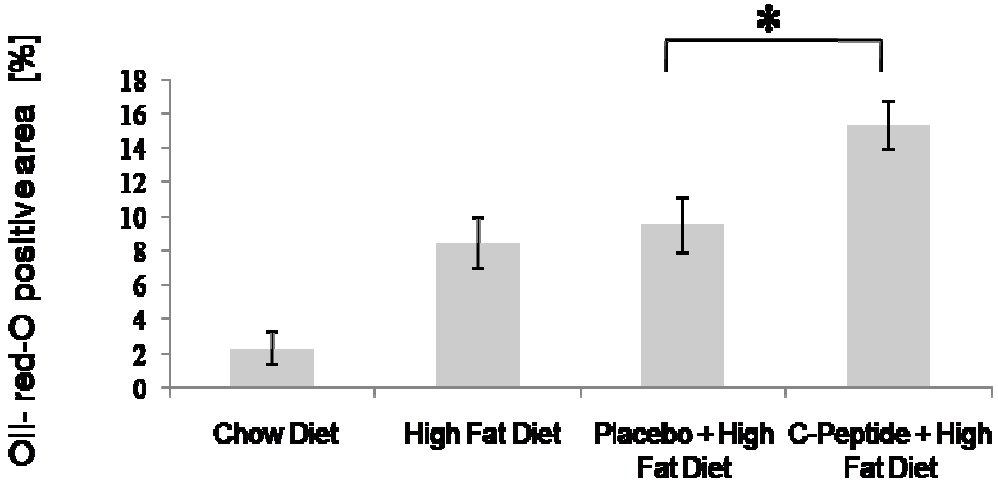

Figure 15. A) C-peptide treatment increases lipid content in aortic arch. Representative sections of aortic arch stained for Oil-red-O in chow diet control mice (a) and high fat diet mice (b). Representative Oil red O–stained sections of aortic arch showed increased Oil-red-O area in C-peptide treated mice (d) compared with placebo (c). **B)** Analysis of Oil-red-O positive areas in percent determined via computer-assisted image quantification. Each data point represents a value from a single mouse. **C)** Diagram represents proportion of lipid content in all four experimental groups (chow diet: n=5, high fat diet: n=8, placebo: n = 17, C-peptide: n = 18). Bars represent mean ± SEM. *P< 0.05

3.6. Effect of C-peptide on plaque formation

There are several ways to access atherosclerosis in mice. Most common is the measurement of lesion development within the arterial tree. The development of atherosclerotic lesions has been quantified after thirteen weeks of cholesterol-rich diet and simultaneous application of C-peptide. The development of atherosclerotic lesions have been observed in all four experimental groups. Figure 16 A represents the distribution of atherosclerotic lesions in mouse aorta. The extent of atherosclerotic lesions has been determined via computer-assisted image quantification and is expressed as percent of total aorta surface. The chow diet group of mice showed only few signs of atherosclerosis in thoracic and abdominal aorta (0.21 ± 0.04%). The placebo and high cholesterol diet control group exhibited moderate extent of Oil-red-O positive area. The C-peptide treated group demonstrated moderate to severe extent of Oil-red-O positive area. Analysis revealed a tendency to an increased atherosclerotic plaque extent in C-peptide treated mice (placebo vs. C-peptide; 3.98 ± 0.5% vs. 5.64 ± 0.69%; P=0.07), however the results did not significantly differ between placebo and C-peptide treated mice.

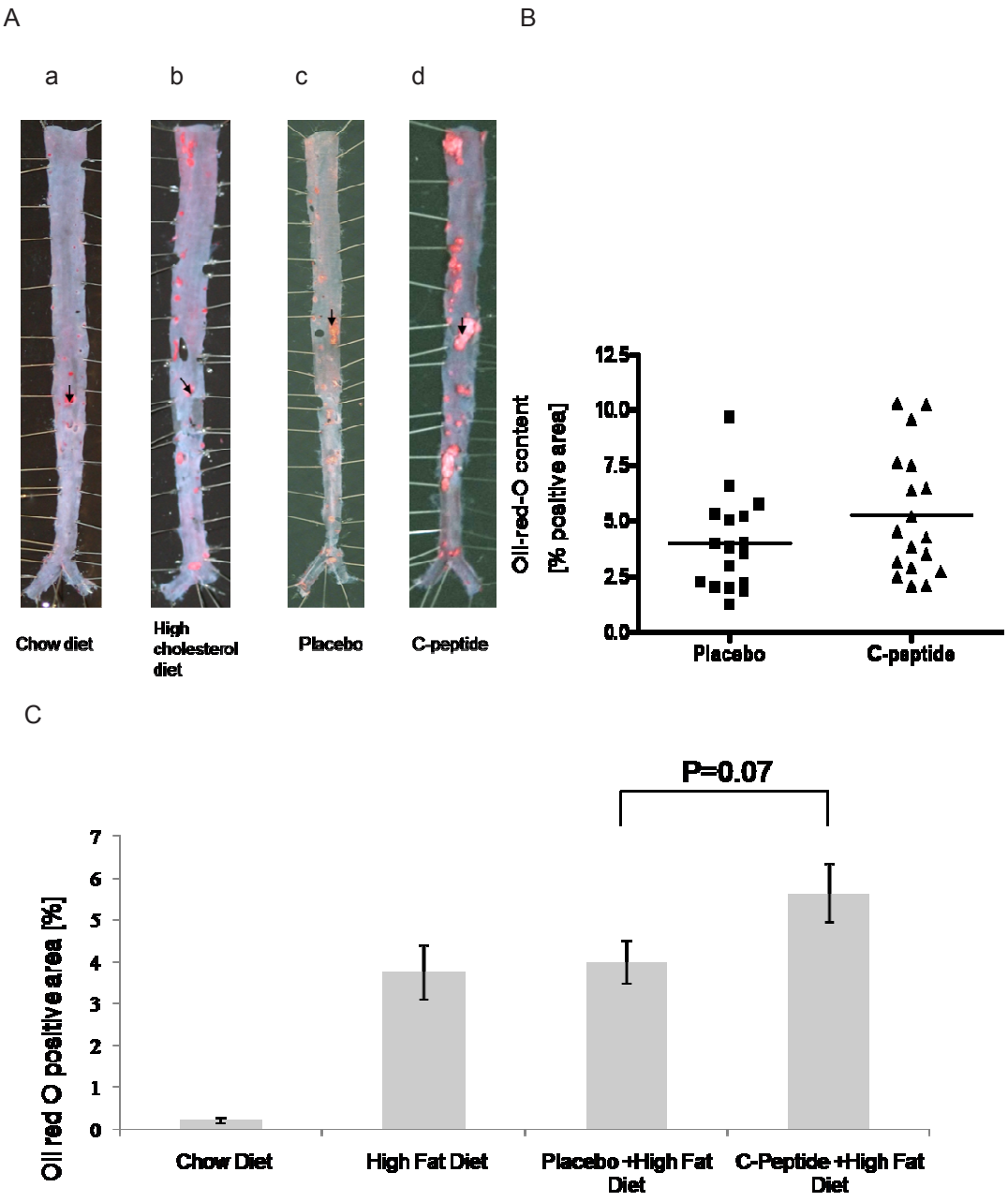

Figure 16. A) C-peptide treatment increases plaque formation in mice. Representative photomicrographs of an aortic specimen stained for lipids with Oil-red-O. Chow diet control group (a), high fat diet control group (b), placebo (c), C-peptide group (d). **B)** Analysis of Oil-red-O positive areas in percent determined via computer-assisted image quantification. Each data point represents a value from a single mouse. **C)** Diagram represents proportion of atherosclerosis in all four experimental groups (placebo: n = 17, C-peptide: n = 18, high cholesterol diet: n=8, chow diet: n=5). Bars represent mean ± SEM. P=0.07

3.7. C-peptide has no effect on collagen content

Additional, structural plaque characteristics have been investigated. Clinical evidence suggests that atherosclerotic plaque components are important predictors of plaque stability and future clinical events. Analysis of collagen positive areas via computer-assisted image quantification determined no difference in collagen extent in placebo and C-peptide group (Figure 17 A, B) (placebo vs. C-peptide; 3.96 ± 0.75% vs. 2.69 ± 0.5% P=0.16). Group of mice on high cholesterol diet demonstrated a similar amount of collagen as a C-peptide group (Figure 17 C, D).

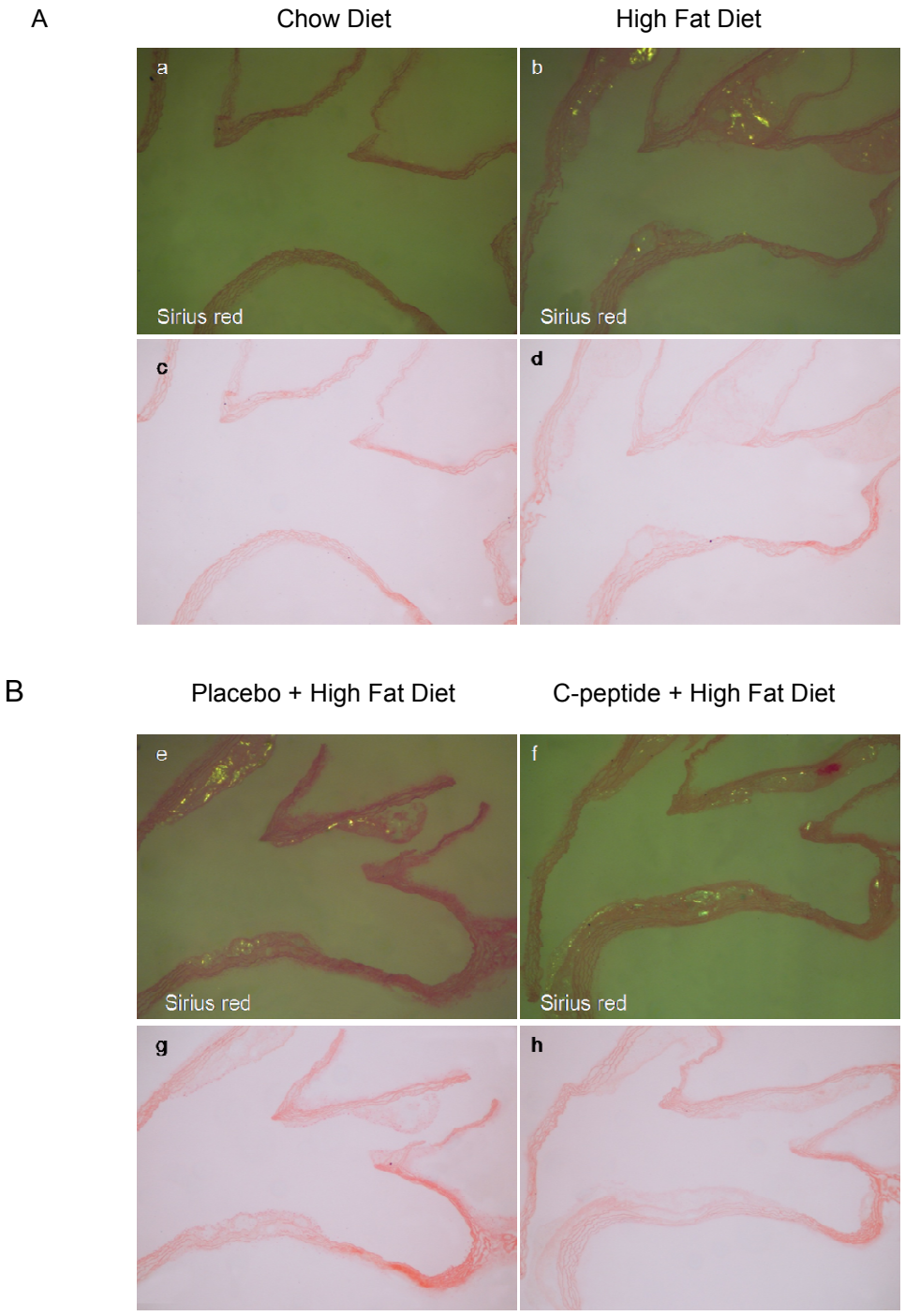

Figure 17. A) Collagen accumulation in longitudinal sections of aortic arch. Picrosirius staining in chow diet and high fat diet mice viewed under polarized light (a) and (b). Photomicrographs on (c) and (d) represent picrosirius staining without polarisation. **B)** Picrosirius red staining viewed under linearly polarized light in the placebo (e) and C-peptide group of mice (f) showed no differences in collagen extent. Picrosirius staining without polarisation on (g) and (h). Yellow colour represents deposition of collagen.

C

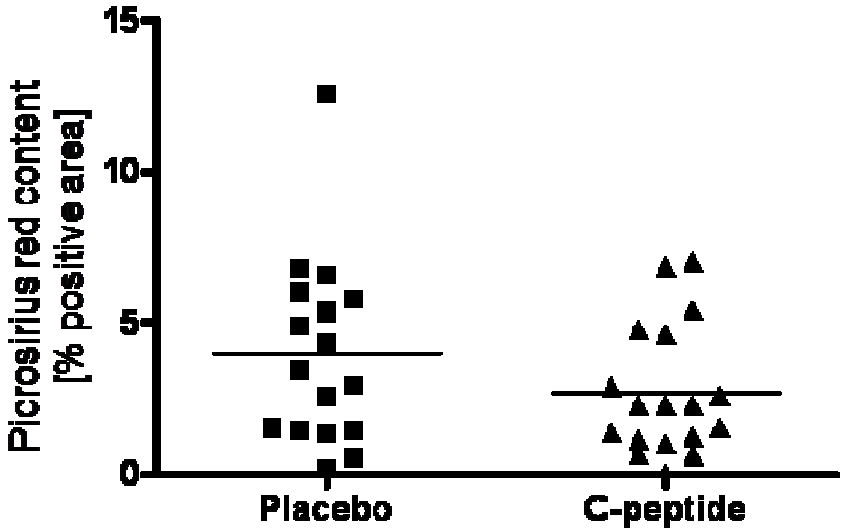

D

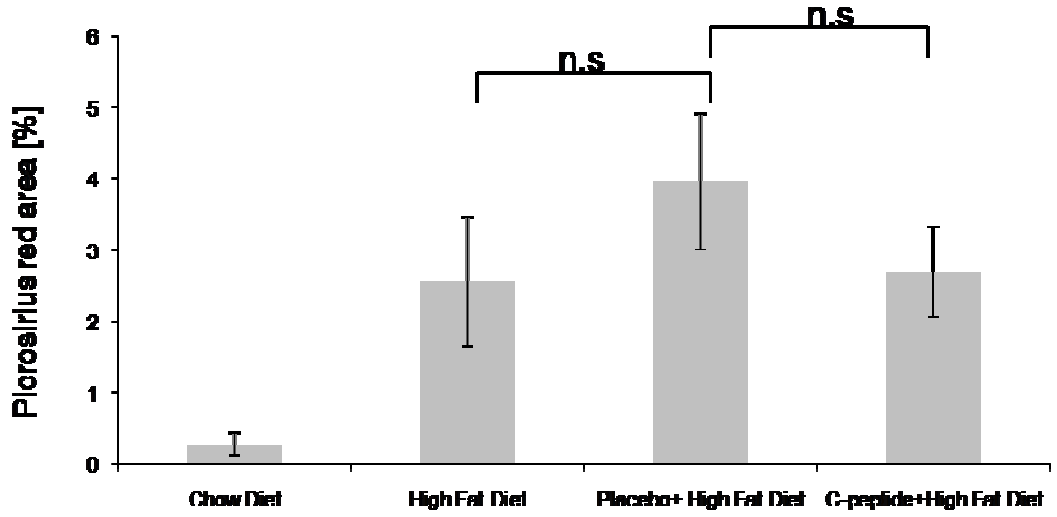

Figure 17. C) Collagen accumulation in longitudinal sections of aortic arch. Analysis of collagen positive areas in percent determined via computer-assisted image quantification. Each data point represents a value from a single mouse. Quantitative analysis of collagen extent in placebo and C-peptide group showed similar amounts of collagen. **D)** Diagram represents collagen positive areas in percent in all four experimental groups. High fat diet group of mice displayed a similar amount of collagen as a placebo and C-peptide. Mice on chow diet exhibited no or little positive areas for collagen (chow diet: n=5, high cholesterol diet: n=8, placebo: n = 17, C-peptide: n = 18). Bars represent mean ± SEM, P=0.16

3.8. C-peptide deposition in aortic sinus

Since the ApoE-deficient hyperholesterolemic mice have been shown to have more extended atherosclerotic lesions in the aortic root than in the aortic arch (Veillard 2004), a second set of immunohistohemical staining has been performed on the aortic sinus. To determine whether any differences exist in C-peptide deposition, smooth muscle cell-, monocyte/macrophage- and collagen content on these two important areas for developing atherosclerosis in mice, cross-sections of aortic sinus have been analysed in the same way as aortic arch sections. Taking into account our previous data, we hypothesized that C-peptide might play a role in the early phase of developing atherosclerosis, meaning we searched for the right time frame for evaluating our experimental groups. The C-peptide deposition in aortic sinus in the placebo and C-peptide group of mice has been analysed. The deposition of C-peptide in atheromas of aortic sinus, determined by computer-assisted image quantification, has been significantly higher in C-peptide group (placebo vs. C-peptide; 10.08 ± 0.83% vs. 13.95 ± 1.4%, $P<0.05$) (Figure 18 A, B).

A

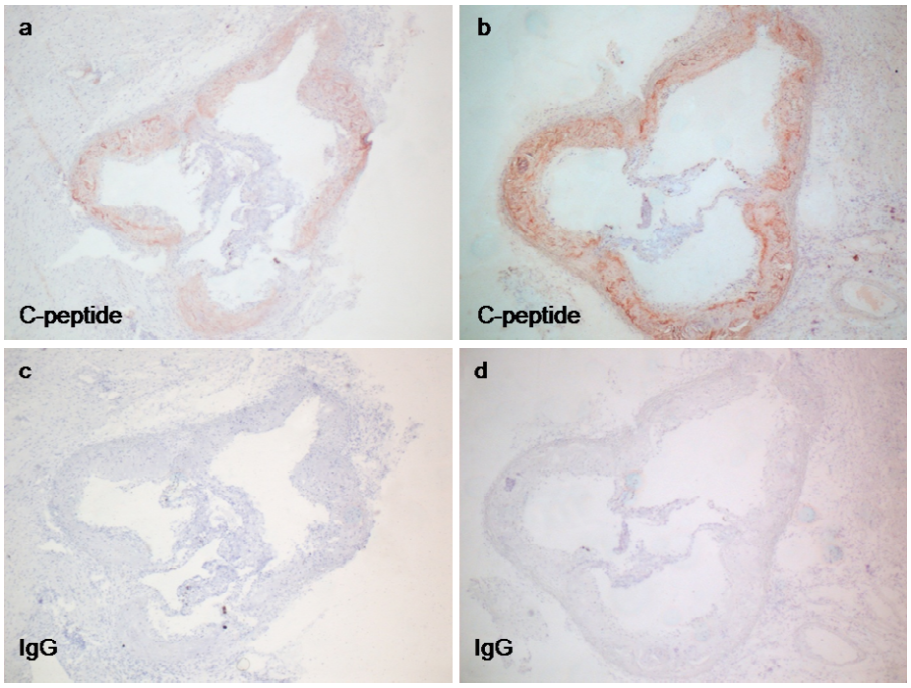

B

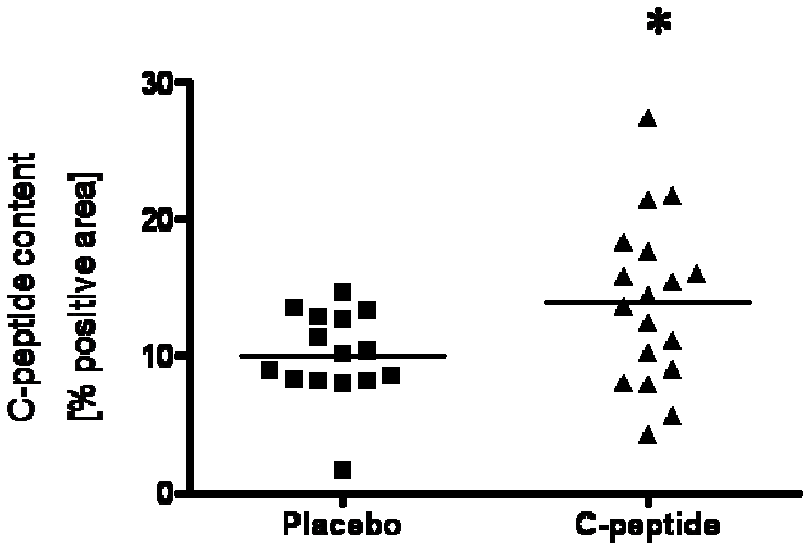

Figure 18. A) C-peptide deposition in aortic sinus. Aortic sinus cross-sections stained with rat-anti-C-peptide antibody demonstrated significantly higher deposition of C-peptide in C-peptide treated mice (b), compared with placebo treated group (a). **B)** Analysis of C-peptide positive areas in percent determined via computer-assisted image quantification. Each data point represents a value from a single mouse. (placebo: n = 15, C-peptide: n = 18) *P<0.05.

3.9. C-peptide increases inflammatory cell content in aortic sinus

To determine if C-peptide treatment besides increased infiltration of monocyte/macrophages in aortic arch causes similar aspects in cross-sections of aortic sinus, slides from placebo and C-peptide treated mice have been stained for monocyte/macrophages. Quantitative analysis showed significantly higher infiltration of monocyte/macrophages in C-peptide treated group of mice (Figure 19 A, B) (placebo vs. C-peptide; 6.85 ± 0.65% vs. 12,87 ± 1.95%, *P<0.05).

A

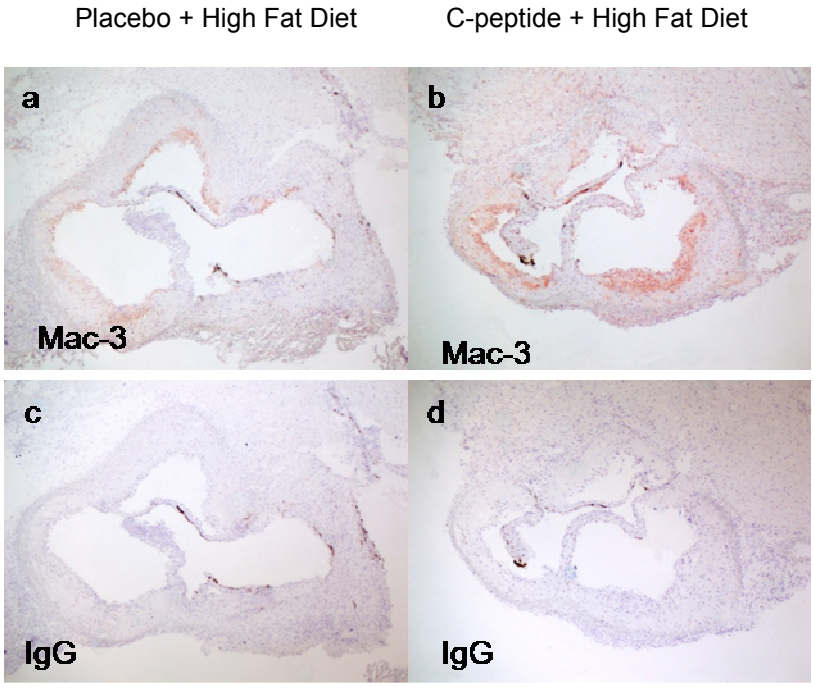

B

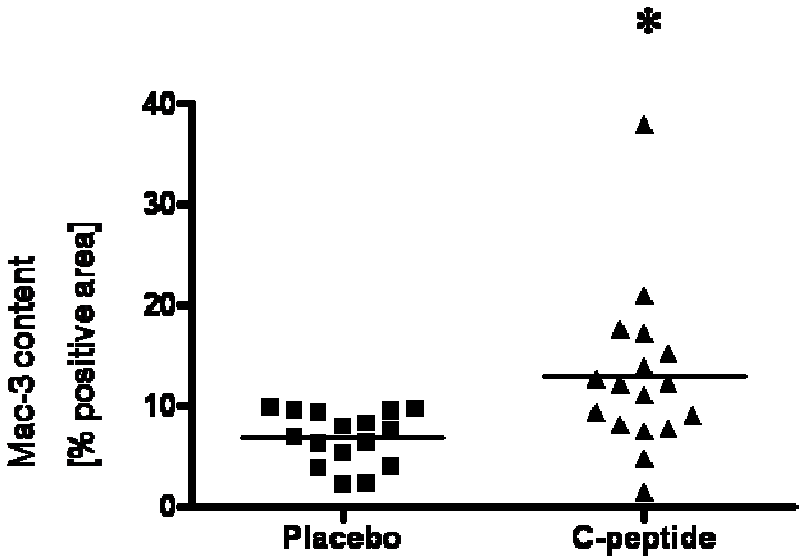

Figure 19. A) C-peptide induces monocyte/macrophages infiltration within the atherosclerotic sinus. Sections represent monocyte/macrophages staining in placebo (a) and C-peptide treated mice (b) after 12 weeks of subcutaneous application of dissolved C-peptide. (c), (d) represent IgG matching controls. **B)** Analysis of Mac-3 positive areas in percent determined via computer-assisted image quantification. Each data point represents a value from a single mouse (placebo: n=16; C-peptide: n=17) *P<0.05

3.10. Effect of C-peptide on the smooth muscle cell content in aortic sinus

It has been already demonstrated that C-peptide treatment increases smooth muscle cell content within the aortic arch in this experimental model. Sections of aortic root have been stained for smooth muscle cells in each mouse. After computer-assisted image quantification it has been determined a similar content of smooth muscle cells in both experimental groups (placebo vs. C-peptide; 5.42 ± 1.21% vs. 7.63 ± 1.5%, P=0.26) (Figure 20 A, B).

A

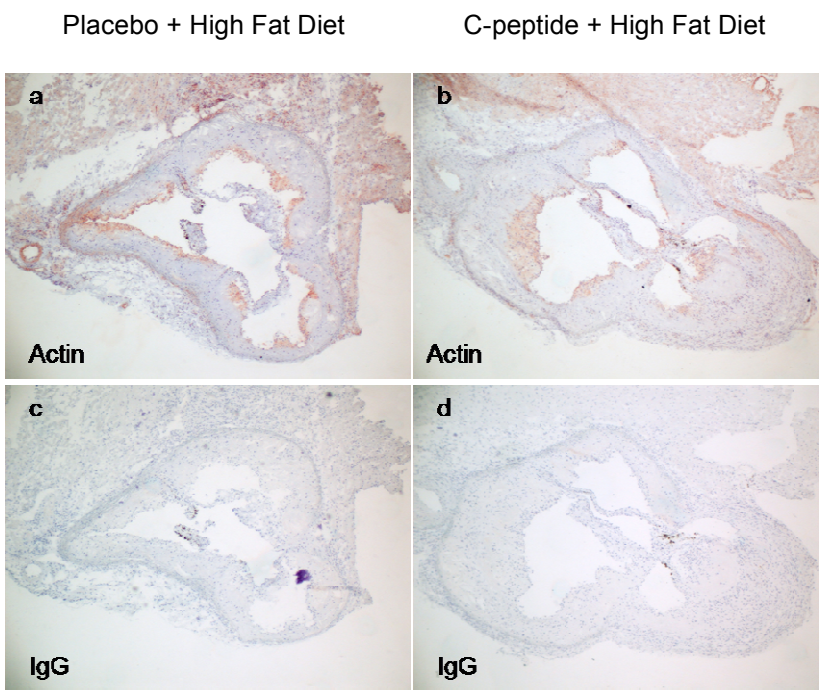

B

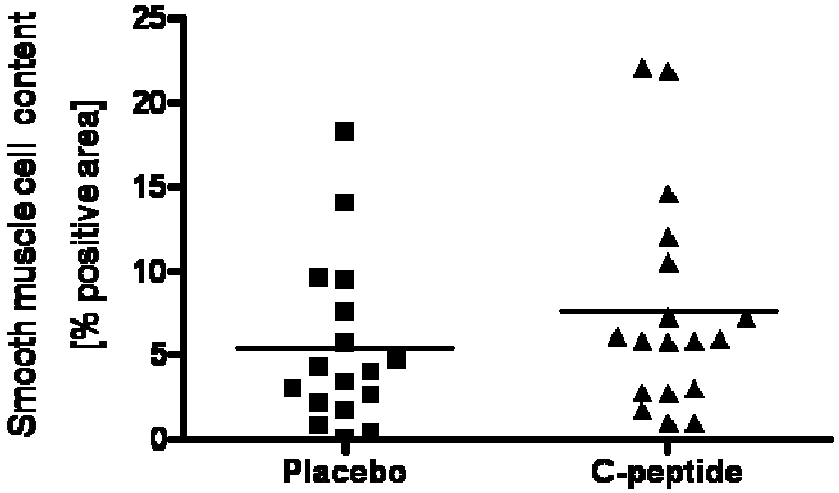

Figure 20. A) Representative cross-sections of aortic sinus stained for smooth muscle cells represents placebo (a) and C-peptide group (b). **B)** Immunohistohemical staining showed similar extent of smooth muscle cells in both experimental groups quantified with computer-assisted image quantification (placebo n=17; C-peptide n=18).

3.11. Effect of C-peptide on the lipid deposition in aortic sinus

The extent of atherosclerosis has been quantified for each mouse in lipid stained aortic arch sections as well as in cross-sections of the aortic sinus. The computer image quantification showed a trend towards increased lipid deposition in C-peptide treated mice at the point of aortic sinus (placebo vs. C-peptide; 45.47 ± 2% vs. 53.58 ± 4.04%, P= 0.08). However, the results did not achieve statistical significance.

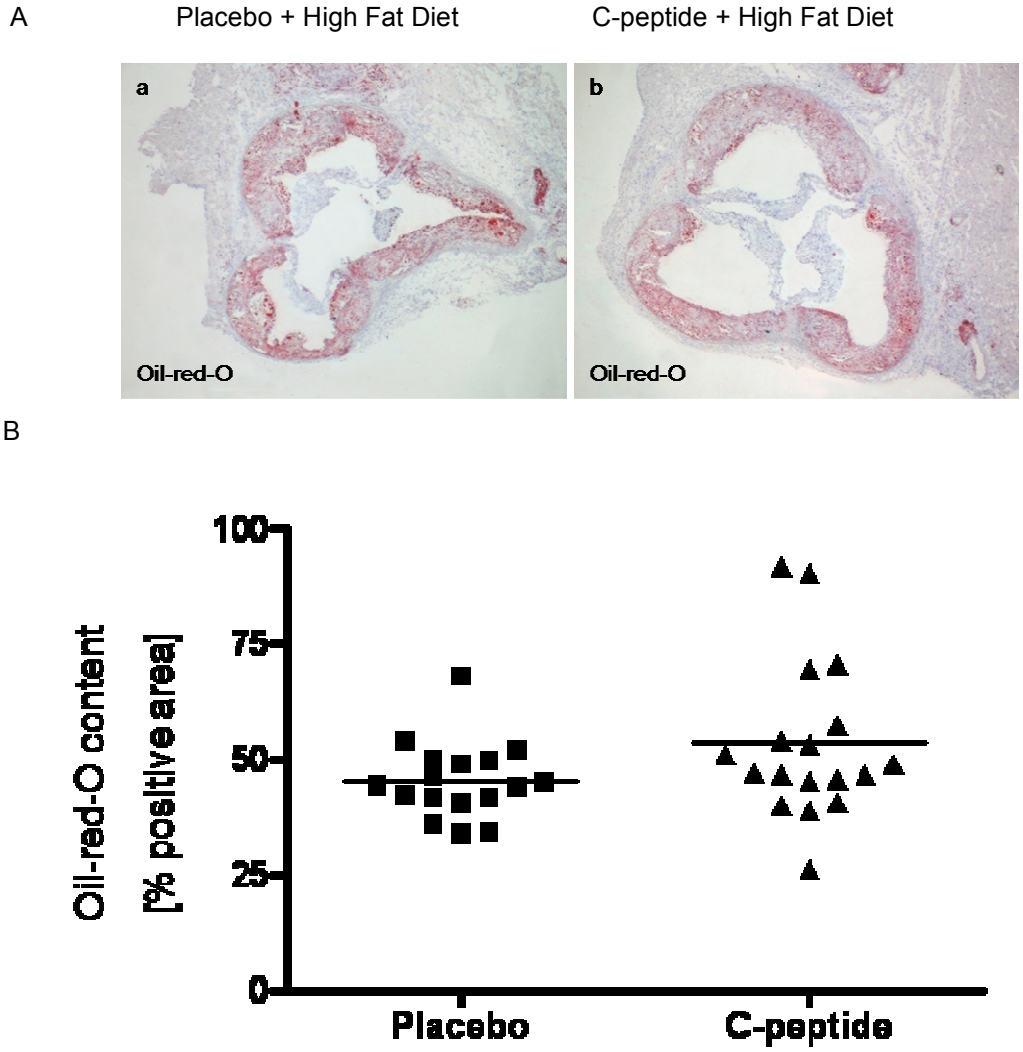

Figure 21. A) C-peptide has no effect on the lipid deposition in aortic sinus. Cross-sections of aortic sinus stained for lipids in placebo (a) and C-peptide group of mice (b). **B)** Analysis of Oil-red-O positive areas in percent determined via computer-assisted image quantification. Each data point represents a value from a single mouse (Placebo: n=17 C-peptide: n=18), P=0.08

4. Discussion

The present study demonstrates that elevated C-peptide concentrations increase inflammatory cell recruitment into the vessel wall in vivo, thus promoting lesion formation in a mouse model of arteriosclerosis. Our findings illustrate for the first time a link between high levels of serum C-peptide and the progression of atherosclerotic lesions in an animal model which until now has been barely visible.

C-peptide is a bioactive molecule

The connecting peptide or C-peptide has been first described by Steiner 1967 as a by-product of insulin biosynthesis. It is produced during insulin biosynthesis and it plays an important biological role in assisting in the arrangement of the correct secondary and tertiary structure of insulin. After identification, early studies searched for an insulin-like function of C-peptide. Since it has not been found (Kitabchi 1977), C-peptide was considered for a long time as a biologically inactive substance. Brandenburg explained in his review that there were two aspects in C-peptide research: C-peptide as an integral part of proinsulin, and C-peptide as an individual entity. Therefore, there were two main directions in the investigations: C-peptide as a diagnostic marker in diabetes mellitus and C-peptide as a bioactive molecule (Brandenburg 2008). Considering C-peptide as a bioactive peptide, the first step was to indentify a receptor for C-peptide. Even if C-peptide specifically binds to cell membranes and activates intracellular signalling pathways (Wahren et al. 2004; Rigler et al. 1999) until now no C-peptide receptor has been identified. Many studies have demonstrated a beneficial effect of C-peptide on the long term complications in type 1 diabetic patients. This might have an important therapeutic implications (Zhong et al. 2004; Wahren et al. 2004), since diabetic complications, for example, decreased blood flow in the extremities, might be prevented by C-peptide (Johansson et al. 2003). Moreover, C-peptide might positively influence diabetic neuropathy via improvements of endoneural blood flow and axonal swelling (Sima et al. 2004). In the kidneys, C-peptide reduced glomerular hyperfiltration and hypertrophy as

well as proteinuria (Samnegard et al. 2007; Nordquist et al. 2007). C-peptide treatment also improves sensory nerve function in early stage type 1 diabetic neuropathy (Ekberg et al. 2007). However, the effects of C-peptide in type 2 diabetic patients as well as on the cell proliferation and apoptosis seem to be a matter of controversy at present. It has not been clarified whether type 2 diabetes mellitus patients suffer from inflammation to a greater extent than type 1 diabetes mellitus patients, but it has been shown that plasma levels of interleukin-6 are associated with C-peptide concentrations in type 2 diabetic patients. (Heliövaara et al. 2005). Furthermore, it has been revealed that C-peptide can prevent vascular dysfunction in diabetic rats (Ido et al. 1997). Kobayasi and colleagues also demonstrated that treatment with C-peptide might suppress hyperproliferation of aortic smooth muscle cells induced by hyperglycemia. Based on the fact that patients with type 2 diabetes mellitus have the same risk of myocardial infarction as nondiabetic subjects with a history of infarction, diabetes has been considered as an atherosclerosis equivalent in CHD (Haffner et al. 1998). The metabolic syndrome, prediabetes and type 2 diabetes mellitus accelerate vascular disease and increase developing of the disease (McNeill et al. 2004). The exact mechanisms for the increased propensity and progression of atherosclerosis in patients with diabetes are unknown. Even if patients with diabetes show more advanced lesion development, the appearance of atherosclerotic lesions are generally similar between patients with and without diabetes (Silva et al. 1995).

C-peptide is present in the vascular wall in ApoE deficient mice

This study demonstrates that high serum levels of C-peptide promote the inflammatory process in the vessel wall in ApoE-deficient mice, thereby leading to increased lesion formation. It has already been shown that C-peptide injections twice daily might induce C-peptide serum levels in mice (Langer et al. 2002). To match their study, we used the same approach for our investigations. In our experimental setting mice were injected subcutaneously with C-peptide and serum levels were measured four hours after injections. The injections were well tolerated without any side effects. Fivefold induction in serum levels of C-peptide

was detectable in C-peptide treated group after twelve weeks of treatment. Since we know that patients with early diabetes and insulin resistance exhibit four to six fold elevated levels of C-peptide, this data suggests that subcutaneous application of C-peptide in ApoE-deficient mice could be an appropriate model to imitate pathophysiological conditions in these patients. C-peptide treatment of these mice did not affect the glucose, insulin or lipid profile compared to control mice. To distinguish the effect of C-peptide on the vessel wall inflammation and plaque formation from potential confusing metabolic effects in diabetes and insulin resistance, we chose the model non-diabetic ApoE-deficient mice (Meir and Leitersdorf 2004), which is a well described model of atherosclerosis. Mice were fed with a high cholesterol diet to induce the development of atherosclerotic lesions (Kolovou et al. 2008).

Previous data from our group showed that C-peptide deposition was found in the intima and media in early atherosclerotic lesions in diabetic patients. In contrast, immunohistochemical staining showed little or no C-peptide staining in non-diabetic subjects. Based on this data we wanted to determine the C-peptide deposition in the vessel wall in mice. Initially this study was designed to show the deposition of C-peptide in the vessel wall in an animal model and subsequently to answer the question whether C-peptide might influence the lesion development. As expected, we found in the placebo as well as in the C-peptide treated group positive areas for C-peptide. A computer-assisted analysis showed significantly higher C-peptide depositions in the atherosclerotic lesions in longitudinal sections of the aortic arch in the group of C-peptide treated mice versus the placebo group. Evaluating the results in Control group 2, which was on the high cholesterol diet for the same duration of time, similar results as in the placebo group has been found. The group of mice on a chow diet showed no or very rare staining for C-peptide in the vessel wall (Figure 11 A). Immunohistochemical staining in cross-sections of aortic root demonstrated similar results (Figure 18 B).

C-peptide induces inflammatory response in ApoE deficient mice

Immunofluorescence staining of diabetic patients in PDAY study showed colocalization of C-peptide with CD4-positive lymphocytes. Parallel sections of atherosclerotic lesions from diabetic patients in the same study showed colocalization of C-peptide with monocyte/macrophages. No similar observations were seen in nondiabetic subjects (Marx 2004). Previous data from our group, using migration assays in modified Boyden chamber revealed that C-peptide induces the migration of monocytes and CD4-positive lymphocytes in concentration dependent manner. Furthermore, these effects of C-peptide were in a range of well established chemokine such as RANTES and MCP-1. Checkerboard analysis demonstrated that C-peptide induces chemotaxis rather than chemokinesis (Marx 2004; Walcher 2004). C-peptide stimulated migration of monocytes and CD4-positive lymphocytes could be inhibited by treating the cells with the PI 3-Kinase inhibitor wortmannin, which suggested the involvement of PI 3-kinase in this process. These results are also in agreement with data of Swiss 3T3 fibroblasts, where C-peptide has been shown to activate PI 3-Kinase (Kitamura et al. 2001). In addition, C-peptide increases the expression of PPAR-γ regulated CD36 scavenger receptor in human THP-1 monocytes (Rasheed et al. 2004). These results also propose that C-peptide besides proatherogenic effects might promote the differentiation of monocyte/macrophages into foam cells. In our experimental setting, the immunohistochemical staining showed significantly higher infiltration of monocyte/macrophages in C-peptide treated mice compared to placebo mice. These data suggest that C-peptide treatment increases monocyte/macrophages content in atherosclerotic lesions. Similar data were also obtained from aortic root cross-sections. Parallel sections of longitudinal aortic arch as well showed colocalization of monocyte/macrophages with C-peptide in ApoE-deficient mice (Figure 13).

Assuming all obtained data we created a potential hypothesis on the role of C-peptide in early atherogenesis. Elevated C-peptide plasma concentration in insulin resistance and type 2 diabetes together with endothelial dysfunction and increased endothelial permeability could lead to a deposition of C-peptide in the

intima of the vessel wall. Many studies demonstrated that endothelial dysfunction occurs early in the insulin-resistant state and is predictive of future cardiovascular events (Hsueh et al. 2004). During a long period of insulin resistance, local concentration of C-peptide in the vessel wall increases and through its chemotactic effect on the monocytes and CD4-positive lymphocytes could provide the migration of these inflammatory cells into the vessel wall.

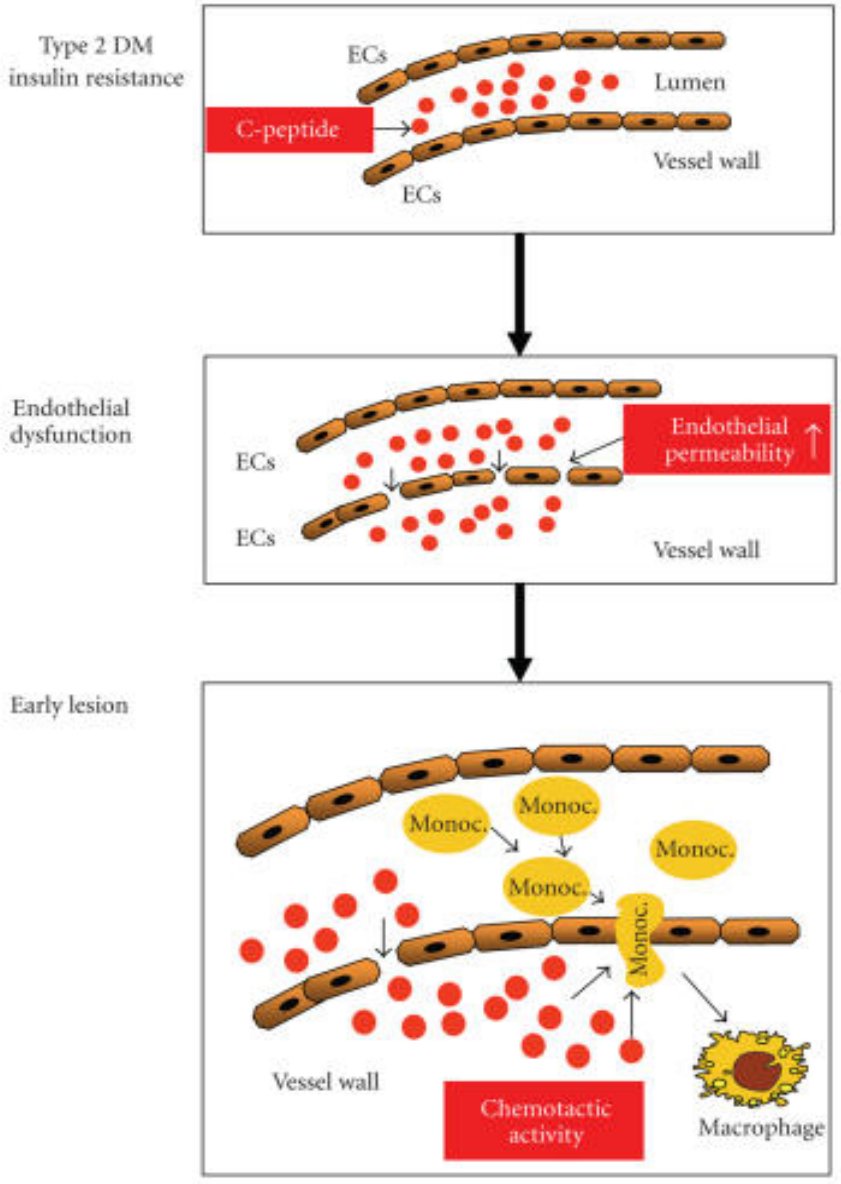

Figure 22. Potential mechanism of C-peptide-induced atherosclerosis.

C-peptide increases smooth muscle cell content in ApoE deficient mice

In advanced atherosclerotic lesions SMCs and their secreted products are major components of the lesion (Stary et al. 1995). It is well established that diabetes accelerates arterial smooth muscle cell proliferation and contributes to a formation of advanced atherosclerotic lesions (Suzuki et al. 2001). It is also known that Insulin resistance and hyperinsulinemia play a key role in supporting SMC proliferation and vascular neointima formation (Park et al. 2001). SMCs are very important in the formation of restenosis after coronary intervention. After vascular injury, these cells start to proliferate and they migrate into the developing neointima. Thus, they become the major cellular substrate of the restenotic tissue (Bittl 1996). Vessel wall injury results in SMCs proliferation in the intimal and medial layer (Hassenstein et al. 1992). Patients with diabetes after arterial injury produced by stent placement have significantly greater incidence of restenosis (Carrozza et al. 1993). In previous studies our group showed colocalization of C-peptide and SMC in the media of the vessel wall in diabetic patients. Furthermore, the biological activity in these cells has been investigated (Walcher 2006). C-peptide stimulation of SMCs induced proliferation of these cells. This was demonstrated by KI-67 nuclear staining in proliferating cells. C-peptide induces several signalling pathways in those cells, including the ERK1/2-MAPK as well as the PI 3-Kinase pathway. C-peptide stimulation in SMCs activates the Src- and PI 3-Kinase and leads to downstream phosphorylation of the MAPK, ERK1/2. Previous work has shown that Src-kinase is involved in LDL induced SMC-proliferation (Cho et al. 2005). ERK1/2 activation plays a major role in cell proliferation and differentiation, especially in SMC proliferation (Velarde et al. 2001). Activation of PI 3-Kinase by C-peptide has been demonstrated in various cell types including vascular cells like monocytes and CD4-positive lymphocytes, suggesting that this signalling molecule plays a critical role in C-peptide induced cell activation in different cell types. Some in vivo studies have demonstrated increase in ERK1/2 activation after balloon catheter injury in animal arteries and inactivation of this pathway has been shown to limit

intimal hyperplasia after a vascular intervention (Liu et al. 2002). In previous in vitro studies C-peptide increased cyclin D1 expression as well as phosphorilation of retinoblastoma protein (Walcher 2006).

The control of smooth muscle cell proliferation by extracellular stimulus takes place in the mid- to late G1 phase where D-type cyclins promote G_1- to S-phase transition by leading to Rb phosphorilation (Harbour et al. 2000; Cho et al. 2005). Data from Walcher and colleagues suggest that C-peptide acts via similar signalling pathways. Interestingly, results from Kobayasi showed opposite results. These results revealed that human C-peptide at high concentrations (100nMol) suppressed the growth of rat SMCs. Proliferation was induced by high glucose and these effects were mediated via inhibition of the PDGF beta receptor/p44/42 MAP Kinases pathway (Kobayashi et al. 2005). Results from our group demonstrated that stimulation with human C-peptide induces a proliferation of human SMCs and rat C-peptide provokes proliferation of rat SMCs. In the present study rat C-peptide increased smooth muscle cell content within the aortic arch in the mouse model, under elevated glucose conditions (Table 3). Control mice on the high fat diet have a similar content of smooth muscle cells under the same glucose conditions. A recent study from Lindahl and colleagues demonstrated that C-peptide is localised to the nucleoli where its promotes transcription of genes encoding for RNA. They showed that C-peptide stimulates the proliferation of chondrocytes and HEK-293 cells. The regulation of ribosomal RNA means that the C-peptide has growth factor activity (Lindahl et al. 2009). Lindahl and colleagues also verified a C-peptide transport into nuclei using labelled peptide. The internalization was followed at 37°C for up to one hour, and was reduced at 4°C after preincubation with pertussis toxin (Lindahl 2007). C-peptide internalization was found in vascular cells, like endothelial cells and vascular smooth muscle cells. C-peptide has been detected as punctuate intracellular structures and these structures were identified as early endosomes. From these results the authors concluded that endosomes could be a signalling station, through which C-peptide might achieve its cellular effects (Luppi et al. 2009).

C-peptide induces plaque formation ApoE deficient mice

The development of atherosclerosis in ApoE-deficient mice takes place in aortic sinus, than at the lesser curvature of the aortic arch, the principal branches of the aorta, and carotid arteries (Reddick et al. 1994; Tangirala et al. 1995). With an increase of age the distribution and size of lesions increase also in the thoracic and abdominal aorta as well as common iliac and femoral arteries. Veillerd and colleagues suggested that the development of atherosclerosis is delayed between the aortic sinus and abdominal aorta in ApoE-deficient mice (Veillerd et al. 2004). The extent of atherosclerotic lesions was measured by lipid deposition stained with Oil-red-O on the aortic sinus, aortic arch and abdominal aorta. First, we compared the aortic arch lipid deposition between placebo and C-peptide group and determined that the results got statistically significant in favour of the C-peptide treated group. The comparison of lipid depositions in the abdominal aorta also indicated a trend in the direction of more lesions in the whole aorta in C-peptide treated mice. The aortic sinus showed also a small trend in lipid content in C-peptide group. A possible explanation for this might be model design since we examined an impact of C-peptide on the top of cholesterol fed animals.

C-peptide has no impact on the plaque stability

The risk of plaque rupture depends on the plaque components. Most ruptures occur in unstable plaques containing a soft lipid-rich core covered by a thin and inflamed cup of fibrous tissue (Takeuchi et al. 2008). A stabile fibrous cap is composed of collagen, synthesized of intimal smooth muscle cells which report the mechanical integrity. The mechanism leading to the plaque instability includes a proteolysis by metalloproteinases. Metalloproteinases are released by activated macrophages and during apoptosis of intimal SMCs, which slow down the collagen synthesis (Newby et al. 1999; Rekhter et al. 2000). A stabile atherosclerotic plaque demonstrates high collagen content, thicker collagen fibers and large numbers of SMCs. In contrast, unstable plaques contain lower collagen content and fiber thickness in atherosclerotic plaques ex vivo (Rekhter

et al. 2000; Deguch et al. 2005; Verhoeven et al. 2006) It was already shown that older ApoE-deficient mice develop advanced unstable atherosclerotic lesions in the brachiocephalic/innominate arteries. These lesions have some of the morphologic features of advanced atherosclerotic lesions in humans, including intra-plaque hemorrhage and calcification (Rosenfeld et al. 2000; Williams et al. 2002). There are a number of studies describing the ApoE-deficient mouse model as useful model to investigate plaque stability and plaque composition (Bea et al. 2002). However, Schwartz and colleagues suggested two potential limitations of murine disrupted plaques: the acute plaque ruptures could be post mortem handling artefacts and buried fibrous cups are an aspect of normal plaque growth (Schwartz et al. 2007). In our study C-peptide impact on a collagen extent has been investigated. Picrosirius staining for collagen in longitudinal sections in aortic arch demonstrated no statistical significance between the placebo and C-peptide group of mice. Under these experimental conditions we can conclude that C-peptide has no influence on the plaque stability.

The majority of data suggest that C-peptide may promote lesion development in patients with type 2 diabetes mellitus and insulin resistance. The application of C-peptide in type 1 diabetic patients who lack C-peptide has been shown to improve diabetic microvasular complications. The potential proatherogenic aspect of C-peptide is not in conflict with the clinical benefits of C-peptide in type 1 diabetes mellitus patients. Comparing the clinical appearance of hypo- and hyperthyroidism where L-thyroxin treatment in hypothyroidism is helpful, but in hyperthyroidism causes different clinical manifestations, C-peptide effects are not contradictory. Similar mechanisms may be applied for C-peptide. In type 1 diabetes C-peptide may be beneficial but in type 2 diabetic patients it can be harmful.

5. Summary

Serum concentrations of C-peptide, a cleavage product of proinsulin, have been found to be elevated in early type 2 diabetes, a high risk population for cardiovascular disease. Recent data from our group revealed deposition of C-peptide in the thoracic artery of diabetic subjects as well as colocalization with CD4-positive lymphocytes and monocyte/macrophages. Furthermore, we demonstrated that C-peptide induces CD4-positive lymphocytes chemotaxis in vitro. Moreover, the potential mechanisms of C-peptide-induced cell migration were elucidate. C-peptide has been also considered as a mitogen of smooth muscle cells in vitro.

However, the present study is the first attempt to investigate in vivo the correlation between high serum levels of C-peptide and the development of atherosclerosis. In an ApoE-deficient mouse model we established constant high serum levels of C-peptide via subcutaneous injections of dissolved peptide for twelve weeks. At the same time mice were on the proatherogenic ‘Western type’ diet to activate lesion development. After analysing immunohistochemical findings, our data revealed a deposition of C-peptide in early atherosclerotic lesions in the aortic arch as well as in the aortic root. These depositions were significantly higher in the group of mice subcutaneously treated with C-peptide (C-peptide group on the high fat diet) compared to the group of mice treated with water (Placebo group on the high fat diet). Furthermore, C-peptide treated mice also exhibited an increased infiltration of monocyte/macrophages on both considered positions, the longitudinal sections of the aortic arch and the cross-sections of the aortic root. Moreover, staining of parallel sections showed a colocalization of C-peptide with monocyte/macrophages in early atherosclerotic lesions. Next, the results from this study revealed that C-peptide treated mice exhibit a higher extent of smooth muscle cells. The increase in monocyte/macrophages as well as smooth muscle cell content in aortic arch in C-peptide mice was followed by an increased accumulation of lipids. These data suggests that the effect of C-peptide on the recruitment of inflammatory cells and proliferation of smooth

muscle cells turns into an increase lesion formation. Furthermore, en-face examination of atherosclerosis in descending aorta demonstrated a trend which is not yet significant in increased lesion formation in C-peptide treated ApoE-deficient mice.

6. Conclusion and future work

This study showed that elevated levels of C-peptide can deposit in the vessel wall in mouse model of atherosclerosis. We managed to establish serum levels of C-peptide which are elevated in the same form like in patients with early diabetes and insulin resistance. The presented data verifies results from our previous studies, thus giving further momentum to the hypothesis that C-peptide may contribute to lesion development in patients with insulin resistance and early type 2 diabetes.

This work can further contribute to the existing knowledge about C-peptide as an active substance. Further studies need to identify a C-peptide receptor. Activating this receptor in type 1 diabetic patients can be beneficial as well as blocking it in type 2 diabetic patients could be of great value in preventing vascular complications.

7. Literature

1. Aleksic, M, Walcher D, Giehl K, Bach H, Grüb M, Durst R, Hombach V. and. Marx N. Signalling processes involved in C-peptide-induced chemotaxis of CD4-positive lymphocytes; *Cell Mol Life Sci*. **66**:1974-84 (2009)
2. An G, Miwa T, Song WL, Lawson JA, Rader DJ, Zhang Y, Song WC. CD59 but not DAF deficiency accelerates atherosclerosis in female ApoE knockout mice. *Mol Immunol*. **46**:1702-9 (2009)
3. Balletshofer B, Rittig K. Enderle M, Volk A, Maerker E; Jacob S Matthaei S, Rett K, Häring H, Endothelial dysfunction is detectable in young normotensive first-degree relatives of subjects with type 2 diabetes in association with insulin resistance. *Circulation*; **101**:1780-178 (2000)
4. Bea F, Blessing E, Bennett B, Levitz M, Wallace E, Rosenfeld M. Simvastatin promotes atherosclerotic plaque stability in ApoE-deficient mice independently of lipid lowering*. Arterioscler Thromb Vasc Biol*. **22**:1832–1837 (2002)
5. Bell FP, Gerrity RG. Evidence for an altered lipid metabolic state in circulating blood monocytes under conditions of hyperlipemia in swine and its implications in arterial lipid metabolism. *Arterioscler Thromb.* **12**:155–162 (1992)
6. Beattie, Duthie, Kwun, Ha, Gordon. Rapid quantification of aortic lesions in apoE(-/-) mice *J Vasc Res*. **46**:347–352 (2009)
7. Beckman JA, Creager MA, Libby P**.** Diabetes and atherosclerosis: epidemiology, pathophysiology, and management. *JAMA*. **287**:2570-2581(2002)
8. Bittl JA. Advances in coronary angioplasty. *The New England Journal of Medicine*. **335**:1290–1302 (1996)
9. Bocan TM, Mueller SB, Mazur MJ, Uhlendorf PD, Brown EQ, Kieft KA The relationship between the degree of dietary-induced hypercholesterolemia in the rabbit and atherosclerotic lesion formation . *Atherosclerosis*. **102**:9-22 (1993)

10. Brandenburg. History and Diagnostic Significance of C-Peptide *Exp Diabetes Res*. 576862 (2008)
11. Buono C, Binder C, Stavrakis G, Witztum J, Glimcher L and Lichtman A. T-bet deficiency reduces atherosclerosis and alters plaque antigen-specific immune responses. *Proc. Natl. Acad. Sci. U. S. A.* **102**:1596–1601 (2005)
12. Buono, C, Pang H, Uchida Y, Libby P, Sharpe A, Lichtman A. B7-1/B7-2 co-stimulation regulates plaque antigen-specific T cell responses and atherogenesis in LDLR-deficient mice. *Circulation.* **109**:2009–2015 (2004)
13. Carrozza JP, Jr, Kuntz RE, Fishman RF, Baim DS. Restenosis after arterial injury caused by coronary stenting in patients with diabetes mellitus. *Annals of Internal Medicine*.**118**:344–349 (1993)
14. Chen L-M, Yang X-W and Tang J-G Acidic residues on the N-terminus of proinsulin C-Peptide are important for the folding of insulin precursor. *J Biochem.* **131**: 855–859 (2002)
15. Cho HM, Choi SH, Hwang KC, Oh SY, Kim HG, Yoon DH, Choi MA, Lim S, Song H, Jang Y, Kim TW. The Src/PLC/PKC/MEK/ERK signaling pathway is involved in aortic smooth muscle cell proliferation induced by glycated LDL. *Mol Cells.* **19**: 60–66 (2005)
16. Cifarelli V, Luppi P, Tse HM, He J, Piganelli J, Trucco M. Human proinsulin C-peptide reduces high glucose-induced proliferation and NF-kappaB activation in vascular smooth muscle cells. *Atherosclerosis*. **201**:248-5 (2008)
17. Clarkson TB, Prichard RW, Morgan TM, Petrick GS, Potvin-Klein K. Remodeling **of** coronary arteries in human and nonhuman primates. *JAMA.* **271**:289-294 (1994)
18. Curtiss LK, Boisvert WA. Apolipoprotein E and atherosclerosis Curr Opin Lipidol. **11**:243-51 (2000)
19. Cybulsky MI, Lichtman AH, Hajra L, Iiyama K. Leukocyte adhesion molecules in atherogenesis. *Clin Chim Acta*. **286**:207-18 (1999)
20. Cybulsky MI, Iiyama K, Li H, Zhu S, Chen M, Iiyama M, Davis V, Gutierrez-Ramos JC, Connelly PW, Milstone DS. A major role for VCAM-

1, but not ICAM-1, in early atherosclerosis *J Clin Invest*. **107**:1255-62 (2001)

21. Dandona P, Chaudhuri A, Ghanim H, Mohanty P. Anti-inflammatory effects of insulin and pro-inflammatory effects of glucose: relevance to the management of acute myocardialinfarction and other acute coronary syndromes. *Rev Cardiovasc Med*. **7**:25-34(2006)
22. Dandona P, Chaudhuri A, Mohanty P, Ghanim H. Anti-inflammatory effects of insulin. *Curr Opin Clin Nutr Metab Care*. **10**: 511-517 (2007)
23. De Fronzo RA. The triumvirate: beta cell, muscle and liver, a collusion responsible for NIDDM. *Diabetes*. **37**: 667-687 (1988)
24. Deguchi J, Aikawa E, Libby P, Vachon J, Inada M, Krane S, Whittaker P, Aikawa M. Matrix metalloproteinase-13/collagenase-3 deletion promotes collagen accumulation and organization in mouse atherosclerotic plaques, *Circulation.* **112**: 2708–2715 (2005)
25. Drobnik J, Dabrowski R, Szczepanowska A, Giernat L, Lorenc J. Response of aorta connective tissue matrix to injury caused by vasopressin - induced hypertension or hypercholesterolemia. *J Physiol Pharmacol.* **51**: 521-533 (2000)
26. Ekberg K, Brismar T, Johansson BL, Lindström P, Juntti-Berggren L, Norrby A, Berne C, Arnqvist HJ, Bolinder J, Wahren J. C-Peptide replacement therapy and sensory nerve function in type 1 diabetic neuropathy. *Diabetes Care.* **30**:71-6 (2007)
27. Engelke K, Halliwill J, Proctor D, Dietz N, Joyner M. Contribution of nitric oxide and prostaglandins to reactive hyperemia in the human forearm. *J Appl Physiol.* **81**: 1807-1814 (1996)
28. Fazio S, Sanan DA, Lee YL, Ji ZS, Mahley RW, Rall SC Jr. Susceptibility to diet-induced atherosclerosis in transgenic mice expressing a dysfunctional human apolipoprotein E (Arg112,Cys142). *Arterioscler Throm*. **14**:1873-9 (1994)
29. Farese RV, Véniant Jr, Cham CM, Flynn LM, Pierott V, Loring JF, Traber M, Ruland S, Stokowski RS, Huszar D, and Young SG. Phenotypic analysis of mice expressing exclusively apolipoprotein B48 or apolipoprotein B100. *ProcNatl Acad Sci USA*. **93**:6393-8 (1996)

30. Finking G and Hanke H. Nikolaj Nikolajewitsch Anitschkow (1885–1964) established the cholesterol-fed rabbit as a model for atherosclerosis research. *Atherosclerosis.* **135**: 1–7 (1997)

31. Gerrity RG. The role of the monocyte in atherogenesis: I. Transition of blood-borne monocytes into foam cells in fatty lesions. Am J Pathol. **103**:181–90 (1981)

32. Gerrity RG. The role of the monocyte in atherogenesis: II. Migration of foam cells from atherosclerotic lesions. Am J Pathol. **103**:191–200 (1981)

33. Green Earl, Coleman Douglas, Kaliss Nathan, Dagg Charles, Russell Elizabeth, Fuller John, Staats Joan, Green Margaret: Biology of the laboratory mouse. DOVER PUBLICATIONS INC., NEW YORK. Second edition. Fig. 7-13 (2007)

34. Gotsman I, Grabie N, Gupta R, Dacosta R, MacConmara M, Lederer J, Sukhova G, Witztum J, Sharpe A, Lichtman A. Impaired regulatory T-Cell response and enhanced atherosclerosis in the absence of inducible costimulatory molecule. *Circulation.* **114**:2047–2055 (2006)

35. Haffner SM, Lehto S, Ronnemaa T, Pyorala K, Laakso M. Mortality from coronary heart disease in subjects with type 2 diabetes and in nondiabetic subjects with and without prior myocardial infarction. *N Engl J Med.* **339**:229–234 (1998)

36. Hansson GK Inflammation, atherosclerosis, and coronary artery disease. *N Engl J Med*. **352**:1685-95. (2005)

37. Harbour JW, Dean DC. Rb function in cell-cycle regulation and apoptosis. *Nat Cell Biol.* **2**: 65–67 (2000)

38. Hassenstein SH, Hanke J, Kamenz M ,Oberhoff S, Hanke R, Riessen KK, Haase E, Betz and Karsch KR**;** Vascular injury and time course of smooth muscle cell proliferation after experimental holmium laser angioplasty. *Circulation***. 86**: 1575-1583 (1992)

39. Heliövaara MK, Teppo AM, Karonen SL, et al. Plasma IL-6 concentration is inversely related to insulin sensitivity, and acute-phase proteins associate with glucose and lipid metabolism in healthy subjects. *Diabetes Obes Metab*. **7**:729–36 (2005)

40. Henriksson, Pramanik A, Shafqat J, Zhong Z, Tally M, Ekberg K, Wahren J, Rigler R, Johansson J, Jörnvall H. Specific Binding of Proinsulin C-Peptide to Intact and to Detergent-Solubilized Human Skin Fibroblasts. *Biochem Biophys Res Commun*. **280**: 423-7 (2001)
41. Horwitz DL, Starr Ji, Mako ME, Blackward WD, Rubenstein AH. Proinsulin, insulin and C-peptide concentrations in human portal and peripheral blood. *J Klin Invest*. **55**: 1278-83 (1975)
42. Hsueh, Lyon, Quiñones**.** Insulin resistance and the endothelium *The American Jurnal of Medicine*. **117**: 109 -117 (2004)
43. Ido Y, Vindigni A, Chang K, Stramm L, Chance R, Heath WF, Di Marchi RD, Di Cera E, Williamson JR. Prevention of vascular and neural dysfunction in diabetic rats by C-peptide. *Science*. **277**:563-6 (1997)
44. Ignatowski AC. Influence of animal food on the organism of rabbits. *S Peterb Izviest Imp Voyenno-Med. Akad*; **16**:154-173 (1908)
45. Ishibashi S, Brown MS, Goldstein JL, Gerard RD, Hammer RE, Herz J. Hypercholesterolemia in low density lipoprotein receptor knockout mice and its reversal by adenovirus-mediated gene delivery*. J Clin Invest.* **92**:883-93 (1993)
46. Ishibashi S, Goldstein JL, Brown MS, Herz J, Burns DK. Massive xanthomatosis and atherosclerosis in cholesterol-fed low density lipoprotein receptor-negative mice. *J Clin Invest*. **93**:1885-93 (1994)
47. Janeway CA Jr, Medzhitov R. Innate immune recognition. *Annu Rev Immunol***. 20**:197-216 (2002)
48. Joannides R, Haefeli W, Linder L, Richard V, Bakkali EH, Thuillez C,. Lüscher TF.Nitric oxide is responsible for flow-dependent dilatation of human peripheral conduit arteries in vivo. *Circulation* **91**:1314-1319 (1995)
49. Jokinen MP, Clarkson TB, Prichard RW. Animal models in atherosclerosis research. *Exp Mol Pathol.* **42**:1–28 (1985)
50. Kitabchi AE. Proinsulin and C-peptide: a review. *Metabolism.* **26**:547-87(1977)
51. Knouff C, Hinsdale ME, Mezdour H, Altenburg MK, Watanabe M, Quarfordt SH, Sullivan PM, Maeda N. Apo E structure determines VLDL

clearance and atherosclerosis risk in mice. *J Clin Invest*. **103**:1579-86 (1999)

52. Kolovou, Anagnostopoulou, Mikhailidis,. Cokkinos. Apolipoprotein E knockout models **14**:338-51 (2008)
53. Kuboki K, Jiang ZY, Takahara N, et al. Regulation of endothelial constitutive nitric oxide synthase gene expression in endothelial cells and in vivo. *Circulation*. **101**:676-681 (2000)
54. Kukhtina NB, Arefieva TI, Krasnikova TL**.** Intracellular signal cascade in CD4+ T-lymphocyte migration stimulated by interferon-gamma-inducible protein-10. *Biochemistry (Mosc)*. **70**:652-656 (2005)
55. Langer S, Born F, Breidenbach A, Schneider A, Uhl E, Messner K. Effect of C-peptide on wound healing and microcirculation in diabetic mice. *Eur J Med Res*. **25**:502-508 (2002)
56. Libby P. Coronary artery injury and the biology of atherosclerosis: inflammation, thrombosis, and stabilization *Am J Cardiol***. 86** 3J-8J (2000)
57. Libby P. Current Concepts of the Pathogenesis of the Acute Coronary Syndromes**.** *Circulation*. **104**:365 - 372 (2001)
58. Libby P, Aikawa M. Stabilization of atherosclerotic plaques: new mechanisms and clinical targets *Nat Med*. **8**:1257-62 (2002)
59. Libby P, Geng YJ, Aikawa M, Schoenbeck U, Mach F, Clinton SK, Sukhova GK, Lee RT Macrophages and atherosclerotic plaque stability. *Curr Opin Lipidol*. **7**:330-5 (1996)
60. Lindahl E, Nyman U, Melles E, Sigmundsson K, Stahlberg M, Wahren J, Obrink B, Shafqat J, Joseph B, Jörnvall H. Cellular internalization of proinsulin Cpeptide. *Cell Mol Life Sci*. **64**:479-486(2007)
61. Lindahl E, Nyman U, Zaman F, Palmberg C, Cascante A, Shafqat J, Takigawa M, Sävendahl L, Jörnvall H, Joseph B. Proinsulin C-peptide regulates ribosomal RNA expression. *J Biol Chem*. [Epub ahead of print] (2009)
62. Liu B, Fisher M, Groves P. Down-regulation of the ERK1 and ERK2 mitogen-activated protein kinases using antisense oligonucleotides inhibits intimal hyperplasia in a porcine model of coronary balloon angioplasty. *Cardiovasc Res*. **54**:640–648 (2002)

63. Luppi P, Geng X, Cifarelli V, Drain P, Trucco M. Cpeptide is internalised in human endothelial and vascular smooth muscle cells via early endosomes. *Diabetologia*. **52**:2218-2228 (2009)

64. Lutgens E, Daemen M, Kockx M, Doevendans P, Hofker M, Havekes L, Wellens H, de Muinck ED. Atherosclerosis in APOE3-Leiden transgenic mice: from proliferative to atheromatous stage. *Circulation*. **99**:276–283 (1999)

65. Javien J, Nastalek P, Korbut R. Mouse models in experimental atherosclerosis. *Journal of physiology and pharmacology*. **55**: 503-517 (2004)

66. Johansson J, Ekberg K, Shafqat J, Henriksson M, Chibalin A, Wahren J and Jörnvall H. Molecular effects of proinsulin C-peptide. *Biochem Biophys Res*. **295**:1035–1040 (2002)

67. Johansson BL, Wahren J, Pernow J. C-peptide increases forearm blood flow in patients with type 1 diabetes via a nitric oxide-dependent mechanism. *Am J Physiol Endocrinol Metab.* **285**:E864–70 (2003)

68. Jormsjö S, Wuttge DM, Sirsjö A, Whatling C, Hamsten A, Stemme S, Eriksson P. Differential expression of cysteine and aspartic proteases during progression of atherosclerosis in apolipoprotein E-deficient mice. *Am J Pathol.* **161**:939-45 (2002)

69. Kinlay S, Libby P, Ganz P. Endothelial function and coronary artery disease. *Curr Opin Lipidol.* **12**: 383–38 (2001)

70. Kitamura T, Kimura K, Jung BD, Makondo K, Okamoto S, Cañas X, Sakane N, Yoshida T and Saito M. Proinsulin C-peptide rapidly stimulates mitogen-activated protein kinases in Swiss 3T3 fibroblasts: requirement of protein kinase C, phosphoinositide 3-kinase and pertussis toxin-sensitive G-protein. *Biochem J*. **355**: 123–129 (2001)

71. Kitamura T, Kimura K, Jung BD, Makondo K, Sakane N, Yoshida T and Saito M. Proinsulin C-peptide activates cAMP response element-binding proteins through the p38 mitogen-activated protein kinase pathway in mouse lung capillary endothelial cells. *Biochem J.* **366**:737-44 (2002)

72. Knouff C, Hinsdale ME, Mezdour H, et al. Apo E structure determines VLDL clearance and atherosclerosis risk in mice. *J Clin Invest*. **103**:1579-86 (1999)

73. Knowles JW, Maeda N. Genetic modifiers of atherosclerosis in mice. *Arterioscler Thromb Vasc Biol.* **20**: 2336–2345 (2000)

74. Kobayashi Y, Naruse K, Hamada Y, Nakashima E, Kato K., Akiyama N, Kamiya H, Watarai A, Nakae M, Oiso Y and Nakamura J. Human proinsulin C-peptide prevents proliferation of rat aortic smooth muscle cells cultured in high-glucose conditions. *Diabetologia* **48**:2396-401 (2005)

75. Mach F, Sauty A, Iarossi AS, Sukhova GK, Neote K, Libby P, Luster AD. Differential expression of three T lymphocyte-activating CXC chemokines by human atheroma-associated cells. *J Clin Invest.* **10**:1041-50 (1999)

76. Mahley R.W, Ji Z.-S. Remnant lipoprotein metabolism: key pathways involving cell-surface heparan sulfate proteoglycans and apolipoprotein E. *J. Lipid Res.* **40**:1-16 (1999)

77. Marx N. Diabetes und Arteriosklerose. *Diabetes und Stoffwechsel*. **4**:205-211(2003).

78. Marx N, Walcher D, Raichle C, Aleksic M, Bach H, Grüb M, Hombach V, Libby P, Zieske, Homma S. Strong J. C-peptide colocalizes with macrophages in early atherosclerotic lesions of diabetic subjects and induces monocytes chemotaxis in vitro. *Arterioscler. Thromb. Vasc. Biol.* **24**:540-545 (2004)

79. Masuda J, Ross R. Atherogenesis during low level hypercholesterolemia in the nonhuman primate. I. Fatty streak formation. *Arteriosclerosis*. **10**:164–77 (1990)

80. Masuda J, Ross R. Atherogenesis during low level hypercholesterolemia in the nonhuman primate. II. Fatty streak conversion to fibrous plaque. *Arteriosclerosis*. **10**:178–87(1990)

81. McNeill AM, Rosamond WD, Girman CJ, Heiss G, Golden SH, Duncan BB, East HE, Ballantyne C. Prevalence of coronary heart disease and carotid arterial thickening in patients with the metabolic syndrome (The ARIC Study). *Am J Cardiol* **94**:1249–1254 (2004)

82. Meir and Leitersdorf. Atherosclerosis in the Apolipoprotein E–Deficient Mouse: A Decade of Progress *Arterioscler Thromb Vasc Biol.* **24**:1006-1014 (2004)

83. Murdoch C, Finn A. Chemokine receptors and their role in inflammation and infectious diseases Blood. **95**:3032-43 (2000)

84. Mutt V and Jorpes J. Structure of porcine cholecystokinin-pancreozymin. *Eur J Biochem* **6**: 156-162 (1968)

85. Nakashima Y, Plump A,. Raines Elaine W,. Breslow Jan L, Ross R. ApoE-Deficient Mice Develop Lesions of All Phases of Atherosclerosis Throughout the Arterial Tree. *Arterioscler Thromb*. **14**:133-40 (1994)

86. Newby A.C. and A.B. Zaltsman. Fibrous cap formation or destruction—the critical importance of vascular smooth muscle cell proliferation, migration and matrix formation, *Cardiovasc Res.* **41**:345–360 (1999)

87. Nordquist L, Moe E, Sjoquist M. The C-peptide fragment EVARQ reduces glomerular hyperfiltration in streptozotocin-induced diabetic rats. *Diabetes Metab Res Rev*. **23**:400–5 (2007)

88. Ohtomo Y, Bergman T, Johansson B-L, Jörnvall H and Wahren J. Differential effects of proinsulin C-peptide fragments on Na^+,K^+-ATPase activity of renal tubule segments. *Diabetologia.* **41**: 287–291(1998)

89. Paigen B, Morrow A, Brandon C, Mitchell D, Holmes P. Variation in susceptibility to atherosclerosis among inbtred strains of mice. *Atherosclerosis*. **57**:65-73 (1985)

90. Paigen B. Genetics of responsiveness to high-fat and high-cholesterol diets in the mouse. *Am J Clin Nutr* **62**:458S-462S (1995)

91. Paigen B, Morrow A, Holmes P, Mitchell D and Williams RA. Quantitative assessment of atherosclerotic lesions in mice. *Atherosclerosis.* **68**:231–240 (1987)

92. Park S-H, Marso SP, Zhou Z, Foroudi F, Topol EJ, Lincoff AM. Neointimal hyperplasia after arterial injury is increased in a rat model of non-insulin-dependent diabetes mellitus. *Circulation*.**104**:815–819 (2001)

93. Piedrahita JA, Zhang SH, Hagaman JR, Oliver PM, Maeda N: Generation of mice carrying amutant apolipoprotein E gene inactivated by gene targeting in embryonic stem cells. *PNAS*. **89**:4471-4475 (1992)

94. Plump AS, Smith JD, Hayek T, Aalto-Setälä K, Walsh A, Verstuyft JG, Rubin EM, Breslow JL: Severe hypercholesterolemia and atherosclerosis

in apolipoprotein E-deficient mice created by homologous recombination in ES cells. *Cell*. **71**:343-53 (1992)

95. Pramanik A, Ekberg K, Zhong Z, Shafqat J, Henriksson M, Jansson O, Tibell A, Tally M, Wahren J and Jörnvall H: C-peptide binding to human cell membranes: importance of Glu27*. Biochem Biophys Res Commun* **284**: 94–98 (2001)
96. Rasheed, Chana, Baines¶, Willars, Brunskill: Ligand-independent activation of peroxisome proliferator-activated receptor-γ by Insulin and C-peptide in kidney proximal tubular cells: dependent on phosphatidylinositol 3-kinase activity. *Jurnal of biological chemistry*. **279**:49747-49754 (2004)
97. Reaven GM: Role of insulin resistance in human disease (syndrome X): an expanded definition. *Annu Rev Med.* **44**:121–131 (1993)
98. Reddick RL, Zhang SH, Maeda: Atherosclerosis in mice lacking apoE. Evaluation of lesional development and progression. *Arterioscler Thromb*. **14**:141-7(1994)
99. Reitman JS, Mahley RW, Fry DL. Yucatan miniature swine as a model for diet-induced atherosclerosis. Atherosclerosis. **43**:119–32 (1982)
100. Rigler R, Pramanik A, Jonasson P, Kratz G, Jansson OT, Nygren P, Ståhl S, Ekberg K, Johansson B, Uhlén S, Uhlén M, Jörnvall H, Wahren J: Specific binding of proinsulin C-peptide to human cell membranes. *Proc Natl Acad Sci*. **96**:13318-23 (1999)
101. Rekhter MD, Hicks GW and. Brammer DW, Hallak H, Kindt E, Chen J, Rosebury W, Anderson M, Kuipers P, Ryan M: Hypercholesterolemia causes mechanical weakening of rabbit atheroma: local collagen loss as a prerequisite of plaque rupture. *Circ Res.* **86** 101–108 (2000)
102. Ross R: Atherosclerosis – an inflammatory disease. *N.Engl. J Med*. **340**:115-26 (1999)
103. Rosenfeld ME, Polinsky P, Virmani R, Kauser K, Rubanyi G, Schwartz SM: Advanced atherosclerotic lesions in the innominate artery of the apoE knockout mouse. Arterioscler Thromb Vasc Biol. **20**:2587–2592 (2000)

104. Royo T, Alfón J, Berrozpe M, Badimon L. Effect of gemfibrozil on peripheral atherosclerosis and platelet activation in a pig model of hyperlipidemia. *Eur J Clin Invest*. **10**:843-52 (2000)

105. Rubenstein A, Clark J, Melani F and Steiner D. Secretion of proinsulin, C-peptide by pancreatic beta cells and its circulation in blood. *Nature* **224**:697-699 (1969)

106. Samnegård B, Jacobson SH, Johansson BL, Ekberg K, Isaksson B, Wahren J, Sjöquist M. C-peptide and captopril are equally effective in lowering glomerular hyperfiltration in diabetic rats. *Nephrol Dial Transplant*. **19**:1385–91(2004)

107. Schwartz SM, Galis Z, Rosenfeld ME, Falk E. Plaque rupture in humans and mice. *Arterioscler Thromb Vasc Biol*. **27**:705-713 (2007)

108. Schwartz CJ, Sprague EA, Kelley JL, Valente AJ, Suenram CA. Aortic intimal monocyte recruitment in the normo and hypercholesterolemic baboon (Papio cynocephalus). An ultrastructural study: implications in atherogenesis. *Virchows Arch A Pathol Anat Histopathol*. **405**:175–91(1985)

109. Shih PT, Elices MJ, Fang ZT, Ugarova TP, Strahl D, Territo MC, et al. Minimally modified low-density lipoprotein induces monocyte adhesion to endothelial connecting segment-1 by activating beta1 integrin. *J Clin Invest*. **103**:613–25 (1999)

110. Silva JA, Escobar A, Collins TJ, Ramee SR, White CJ. Unstable angina. A comparison of angioscopic findings between diabetic and nondiabetic patients. *Circulation* **92**:1731–1736 (1995)

111. Sima AA, Zhang W, Grunberger G. Type 1 diabetic neuropathy and C-peptide. *Exp Diabesity Res*. **5**:65–77 (2004)

112. Sjoland H, Eitzman DT, Gordon D, Westrick R, Nabel EG, Ginsburg D. Atherosclerosis progression in LDL receptor-deficient and apolipoprotein E-deficient mice is independent of genetic alterations in plasminogen activator inhibitor-1. *Arterioscler Thromb Vasc Biol*. **20:**846–852 (2000)

113. Skalen K, Gustafsson M, Rydberg EK, Hulten LM, Wiklund O, Innerarity TL, Boren J. Subendothelial retention of atherogenic lipoproteins in early atherosclerosis. *Nature*; **417**:750–4 (2002)

114. Smith JD, Breslow JL. The emergence of mouse models of atherosclerosis and their relevance to clinical research. *J.Intern Med*. **242**:99-109 (1997)

115. Stary HC, Chandler AB, Dinsmore RE, Fuster V, Glagov S, Insull W, Jr, Rosenfeld ME, Schwartz CJ, Wagner WD, Wissler RW. A definition of advanced types of atherosclerotic lesions and a histological classification of atherosclerosis : a report from the Committee on Vascular Lesions of the Council on Arteriosclerosis, Am Heart Association. *Circulation*. **92**:1355–1374 (1995)

116. Steiner D, Cunningham D, Spigelman L, and Aten B. Insulin biosynthesis: evidence for a precursor. *Science* **157**:697-700 (1967)

117. Strong JP, Bhattacharyya AK, Eggen DA, Stary HC, Malcom GT, Newman WP III, Restrepo C. Long-term induction and regression of diet-induced atherosclerotic lesions in rhesus monkeys, II: morphometric evaluation of lesions by light microscopy in coronary and carotid arteries. *Arterioscler Thromb.* **14**:2007-2016 (1994)

118. Sullivan PM, Mezdour H, Aratani Y, Knouff C, Najib J, Reddick RL, Quarfordt SH, Maeda N. Targeted replacement of the mouse apolipoprotein E gene with the common human APOE3 allele enhances diet-induced hypercholesterolemia and atherosclerosis. *J Biol Chem*. **272**:17972-80 (1997)

119. Sullivan PM, Mezdour H, Quarfordt SH, Maeda N.Type III hyperlipoproteinemia and spontaneous atherosclerosis in mice resulting from gene replacement of mouse Apoe with human Apoe2. *J Clin Invest*. **102**:130-5 (1998)

120. Suzuki LA, Poot M, Gerrity RG, Bornfeldt KE. Diabetes accelerates smooth muscle accumulation in lesions of atherosclerosis: lack of direct growth-promoting effects of high glucose levels. Diabetes. **50**:851–860 (2001)

121. Takeuchi, Takuji Ohigashi, Kunio Shinohara, Seinosuke Kawashima, Mitsuhiro Yokoyama, Hirata, Momose, Atherosclerotic plaque imaging using phase-contrast X- *Am J Physiol Heart Circ Physiol* **294**:H1094–H1100 (2008)

122. Tangirala RK, Rubin EM, Palinski W. Quantitation of atherosclerosis in murine models: correlation between lesions in the aortic origin and in the entire aorta, and differences in the extent of lesions between sexes in LDL receptor-deficient and apolipoprotein E-deficient mice. *J Lipid Res.* **36**:2320–2328 (1995)

123. Trovati M, Anfossi G**.** Influence of insulin and of insulinresistance on platelet and vascular smooth muscle cell function. *J Diabetes Complications*. **16**:35-40 (2002)

124. Velarde V, Jenkins AJ, Christopher J, Lyons TJ, Jaffa AA. Activation of MAPK by modified low-density lipoproteins in vascular smooth muscle cells. *J Appl Physiol.* **91**:1412–1420 (2001)

125. Veillard NR, Steffens S, Burger F, Pelli G, Mach F. Differential expression patterns of proinflammatory and antiinflammatory mediators during atherogenesis in mice. *Arteriosclerosis, Thrombosis, and Vascular Biology.* **24**:2339 (2004)

126. Veniant MM, Pierotti V, Newland D, et al. Susceptibility to atherosclerosis in mice expressing exclusively apolipoprotein B48 or apolipoprotein B100. *J Clin Invest*. **100**:180-8 (1997)

127. Verhoeven, de Vries; Pasterkamp; R Ackerstaff,. Schone;veld, Velema, de Kleijn; Carotid atherosclerotic plaque characteristics are associated with microembolization during carotid endarterectomy and procedural outcome moll. *Stroke*. **36:**1735-1740 (2006)

128. van Vlijmen BJ, van den Maagdenberg AM, Gijbels MJ, Van Der Boom H, Hogen Esch H, Frants RR, Hofker MH, Havekes LM. Diet-induced hyperlipoproteinemia and atherosclerosis in apolipoprotein E3-Leiden transgenic mice. *J Clin Invest.* **93**:1403–1410 (1994)

129. van Ree JH, van den Broek WJ, Dahlmans VE, Groot PH, Vidgeon-Hart M, Frants RR, Wieringa B, Havekes LM, Hofker MH. Diet-induced hypercholesterolemia and atherosclerosis in heterozygous apolipoprotein E-deficient mice. *Atherosclerosis.* **111**:25-37 (1994)

130. Wahren J, Ekberg K, Jörnvall H. C-peptide is a bioactive peptide. *Diabetologia* **50**:503-9 (2007)

131. Wahren J, Shafqat J, Johansson J, Chibalin A, Ekberg K, Jörnvall H. C-peptide stimulates ERK1/2 and JNK MAP kinases via activation of protein kinase C in human renal tubular cells. *Exp Diabesity Res.* **5**:15-23 (2004)

132. Wahren J, Shafqat J, Johansson J, Chibalin A, Ekberg K, Jörnvall H. Molecular and cellular effects of C-peptide--new perspectives on an old peptide. *Exp Diabesity Res*. **5:**15-23 (2004)

133. Walcher D, Aleksic M, Jerg V, Hombach V, Zieske A, Homma S, Strong J, Marx N: C-peptide induces chemotaxis of human CD4-positive cells: involvement of pertussis toxin-sensitive G-proteins and phosphoinositide 3-kinase. Diabetes **53**:1664-70 (2004)

134. Walcher D, Babiak C, Poletek P, Rosenkranz S, Bach H, Betz S, Durst R, Grüb M, Hombach V, Strong J, Marx N: C-Peptide induces vascular smooth muscle cell proliferation: involvement of SRC-kinase, phosphatidylinositol 3-kinase, and extracellular signal-regulated kinase 1/2. *Circ Res* **99**:1181-7 (2006)

135. Wheatcroft SB, Williams IL, Shah AM and Kearney MT. Pathophysiological implications of insulin resistance on vascular endothelial function. *Diabet Med*. **20**:255-68 (2003)

136. Whitman S. A practical approach to using mice in atherosclerosis research. *Clin Biochem Rev.* **25**:81-93 (2004)

137. Williams H, Johnson JL, Carson KG, Jackson CL, Characteristics of intact and ruptured atherosclerotic plaques in brachiocephalic arteries of apolipoprotein E knockout mice. *Arterioscler Thromb Vasc Biol*. **22**:788–792 (2002)

138. Yan ZQ, Hansson GK. Innate immunity, macrophage activation, and atherosclerosis. *Immunol Rev*. **219**:187–203 (2007)

139. Yuri V. Bobryshev**.** Monocyte recruitment and foam cell formation in atherosclerosis. *Micron*. **37**:208-22 (2006)

140. Zeiher AM, Goebel H, Schächinger V, Ihling C. Tissue endothelin-1 immunoreactivity in the active coronary atherosclerotic plaque. A clue to the mechanism of increased vasoreactivity of the culprit lesion in unstable angina. *Circulation*. **91**:941-7 (1995)

141. Zernecke A, Shagdarsuren E, Weber C. Chemokines in atherosclerosis: an update. *Arterioscler Thromb Vasc Biol.* **28**:1897–1908 (2008)

142. Zhang SH, Reddick RL, Burkey B, Maeda N. Diet-induced atherosclerosis in mice heterozygous and homozygous for apolipoprotein E gene disruption. *J Clin Invest*. 94:937-45 (1994)

143. Zhang SH, Reddick RL, Piedrahita JA, Maeda N. Spontaneous hypercholesterolemia and arterial lesions in mice lacking apolipoprotein E. *Science*. **258**:468-71(1992)

144. Zhong Z, Kotova O, Davidescu A, Ehrén I, Ekberg K, Jörnvall H, Wahren J, Chibalin AV. C-peptide stimulates Na+, K+-ATPase via activation of ERK1/2 MAP kinases in human renal tubular cells. *Cell Mol Life Sci*. **61**:2782-90 (2004)

Acknowledgments

I would like to dedicate this dissertation to my late grandfather Dusan Arsic who believed in diligence, science, art, and the pursuit of academic excellence.

This project would not have been possible without the support of many people.

First, I would like to thank to Prof. Dr. Vinzenz Hombach for the possibility to perform my thesis in the Department of Internal Medicine 2.

I especially want to thank to my supervisor Prof. Dr. Nikolaus Marx whose support and guidance made my thesis work possible. He has been actively interested in my work and has always been available to advise me. I am very grateful for his patience, motivation and enthusiasm.

I also thank to Research training group GRK 1041 and Prof. Dr. Bernhard Böhm for introducing always exciting research topics and for valuable discussions about specific scientific problems.

I wish to express my warm and sincere thanks to PD. Dr. Daniel Walcher without whose knowledge and assistance this study would not have been successful.

Looking back, I have to express my gratitude to Renate, Angelina and Helga for helping me learning many new techniques and for the pleasant working atmosphere.

My special thanks goes to my colleague Philipp Heinz for being the ultimate lab neighbour, for his friendship, his help and chats.

My very warm thanks goes to dear friend Ivana, for invaluable help with my child, for being my very best friend and the best babysitter ever.

I owe a special thanks also to my sister and my parents for their permanent support and understanding.

At least, I'm eternally grateful to my son Stefan for being the best child at critical time. Without him, and his ability to raise my spirits when I was most discouraged, I could never made it this far.